A Thesis for the Degree of Master of Science

# Internal microstructures of amylopectin and their contribution to the physical properties of waxy-cereal starches

찰곡류 녹말의 아밀로펙틴 내부 미세구조가
녹말의 물리적 특성에 미치는 영향

February 2015

Yun, Won Jun

Department of Agricultural Biotechnology

Seoul National University

농학석사학위논문

# Internal microstructures of amylopectin and their contribution to the physical properties of waxy-cereal starches

## 찰곡류 녹말의 아밀로펙틴 내부 미세구조가 녹말의 물리적 특성에 미치는 영향

지도교수 문 태 화
이 논문을 석사학위 논문으로 제출함

2015년 2월
서울대학교 대학원
농생명공학부
윤 원 준

윤 원 준의 석사학위 논문을 인준함
2015년 2월

위 원 장 유 상 렬 인

부위원장 문 태 화 인

위 원 최 상 호 인

A Thesis for the Degree of Master of Science

# Internal microstructures of amylopectin and their contribution to the physical properties of waxy-cereal starches

by

**Yun, Won Jun**

**Advisor: Tae Wha Moon, Professor**

Submitted in Partial Fulfillment of the Requirement
for the Degree of Master of Science

**February 2015**

**Department of Agricultural Biotechnology**

**Seoul National University**

# ABSTRACT

Amylopectin, one of the two major components of starch, is known as an assemblage of molecular arrangement of a cluster. In this study, typical A-type starches, waxy corn, waxy rice, waxy barley, and waxy wheat starch, were partially hydrolyzed to isolate the clusters using α-amylase. These clusters were further hydrolyzed to the building blocks, small and tightly branched units of the amylopectin, and analyzed to figure out the characteristics of internal microstructure of amylopectin. This study aimed to investigate the effects of internal microstructure of amylopectin on the physical properties, such as relative crystallinity, thermal, pasting, and rheological properties.

The degree of polymerization of clusters where external residues had been removed by phosphorylase and β-amylase was similar to each other, and the a- to b-chain ratio ranged from 1.11 for waxy corn starch to 1.40 for waxy barley starch. The internal-microstructural properties of four waxy-cereal starches were categorized into two types. Waxy corn and waxy rice starches presented a relatively small amount of building blocks, a smaller density, and long inter-block chain length in clusters. Meanwhile, waxy barley and waxy wheat starches were composed of a large amount of building blocks, and

showed a higher density and shorter inter-block chain length in clusters. Therefore, a difference in the arrangement of double helices in crystalline lamellae was predicted. The disordered double helix content estimated by X-ray and $^{13}C$ CP/MAS NMR was lower in waxy corn and waxy rice starches, but was higher in waxy barley and waxy wheat starches. This result indicated that external double helices of amylopectin of waxy barley and waxy wheat starches were disorderly arranged because large number of building blocks were connected by short distance in internal chains of amylopectin. In onset and peak temperatures determined by differential scanning calorimetry, earlier gelatinization of disordered double helices was observed. Differences were also shown in pasting temperature derived from Rapid Visco Analyzer and viscoelasticity measured by rheometery.

In conclusion, the density of building blocks and chain length between building blocks in amorphous lamellae can affect the arrangement of double helices in crystalline lamellae and the internal microstructure of amylopectin can cause different physical properties of starch.

**Keywords:** waxy-cereal starch, amylopectin, amorphous lamellae, internal microstructure, cluster, building block, physical properties

**Student Number: 2013-21177**

# ABBREVIATIONS

DP: degree of polymerization

CL: chain length

LD: limit dextrin

NC: number of chain

NBB: number of building blocks

IB-CL: inter-block chain length

WCS: waxy corn starch

WRS: waxy rice starch

WBS: waxy barley starch

WWS: waxy wheat starch

# CONTENTS

# List of tables

# List of figures

# INTRODUCTION

Starch, one of the most important carbohydrates as an energy source for human, is an abundant nutrient in our food raw materials, such as rice, wheat, corn, and potato. Starch is a homopolysaccharide composed of glucose and can be separated into amylose and amylopectin based on the structure. Amylose consists of glucose units joined by α-(1,4) glycosidic bonds, resulting in a linear chain and amylopectin forms as glucose units are connected using α-(1,4) and α-(1,6) linkages, making a branched structure. The ratio of amylose to amylopectin and branch structure of amylopectin linked by α-(1,6) bonds vary depending on the source of the starches (Bates et al., 1943). Most of the starches have more amylopectin than amylose, and thus amylopectin greatly affects the properties of the starch (Jane et al., 1999; Sasaki et al., 2000).

Amylopectin consists of clusters, which are a bundle of branched chains formed by double helix. The model of the cluster structure of amylopectin was introduced based on the structural studies of acid-treated starch granules (Kainuma & French, 1972). Such treatment results in a highly crystalline product containing mostly short chains from amylopectin (Jenkins & Donald, 1997). As the acid removed the branches as well as a large portion of the

amorphous layers in the granules, it was suggested that the branches were mostly clustered into the amorphous lamellae (Robin, 1974). The cluster was estimated that a single, large amylopectin macromolecule with degree of polymerization (DP) in the order of 10–16 $x10^3$ is built from 60 to 120 units (U) of clusters (Takeda et al., 2003). These clusters organize the crystalline lamella (the layer of double helix) and amorphous lamella (branched part of cluster), and these two lamellae are included in semicrystalline shell. Starch granules are made up of alternating amorphous and semicrystalline shells, between 100 and 800 nm thick (Waigh et al., 1997). These structures are termed growth rings. Recently, high-tech equipments are introduced to investigate starch structure. In the semicrystalline region, the nanoscopic lamellae are parallel to the surface of the starch granule as analyzed with X-ray beams at a synchrotron (Chanzy et al., 2006). In addition, atomic force microscopy showed the presence of blocklets within growth rings at the starch granule's surface (Gallant et al., 1997). However, no further details are known about these structures and it is still unclear how these units and growth rings relate to each other.

There are specific enzymes used for structural analysis of amylopectin by hydrolyzing the starch. α-Amylases hydrolyze starch endo-wise at inner α-(1,4) linkages and rapidly reduce viscosity and iodine coloration (blue value) with a gradual increase in reducing value. Especially, liquefying α-amylase

of *Bacillus subtilis* or *B. amyloliquefacience* attacks at external chains resulting in linear dextrins (mostly of DP 6–7) (Bertoft, 1989a; Robyt & French, 1963). The enzyme has nine subsites distributed around the catalytically active site. When all subsites are filled with glucose residues, the reaction is fast, and if not filled, the rate of the hydrolysis decreases considerably (Robyt & French, 1963). Thus, clusters are considered to be formed after the first, rapid stage of hydrolysis. At this point, the reaction is stopped, and the clusters are collected by precipitation in methanol (Bertoft & Spoof, 1989). The most commonly used exo-enzyme is β-amylase, which attacks amylopectin from the non-reducing ends and produces maltose. The enzyme cannot bypass the branches, and therefore a β-limit dextrin (LD) remains that contains all branches and the entire internal part of the macromolecule. As a result, the chains of β-LD are reduced into glucose, maltose, or maltotriose stubs, depending on the type of the chain and even and odd number of the original chain (Bertoft et al., 2008). Another exo-enzyme is phosphorylase *a* from rabbit muscle. This enzyme produces glucose 1-phosphate and shortens the chain length of the amylopectin (Steup, 1988). Both isoamylase and pullulanase are debranching enzymes that hydrolyze α-(1,6) glucosidic linkages in starch resulting in linear chains (Harada et al., 1972).

Amylopectin chains are classified into A-, B-, and C-chain. (Peat et al.

(1952). A-chain is linear, unsubstituted by other chains and connected through (1→6)-α-linkages, whereas B-chain carries other chain (A-chain or other B-chain). The single C-chain has the sole reducing end, but is similar to the B-chain. The B-chains contain an external chain, which extends from the outmost branch to the non-reducing end of the chain, and the rest of the internal chain. By phosphorylase *a*, amylopectin is hydrolyzed to φ-LD containing A-chains in the form of maltotetraose stubs, and the external B-chain segments have maltotriose stubs if the original chain contains an even or odd number of residues (Bertoft, 1989b). If the φ-LD is treated with β-amylase, one maltose is released from each external chain stub. All A-chains are therefore represented by maltose stubs in the resulting φ,β-LD, whereas all external segments of the B-chains are glucose stubs (Bertoft, 1989b). The φ,β-LD can provide important information about the internal structure of amylopectin without an effect of its original chain length by removal of external chain, and when it is debranched, the A- to B-chain ratio can be estimated.

The branches are apparently not evenly distributed within the clusters, but found in small groups. These the smallest, tightly branched units of the amylopectin is called building block and can be isolated from clusters by an extensive hydrolysis (Bertoft et al., 2012a). Since the internal chain segments inside the clusters are hydrolyzed very slowly, building blocks are isolated

by 100–200 times higher enzyme concentration than is used for cluster isolation (Bertoft et al., 1999). The size of the building blocks varies from DP 5-40 and classified into group 2 to 7 depending on estimated number of chains (NC). Group 2 consists of only two chains and, three to seven chains compose group 3 to 7, respectively (Bertoft, 2007a). Based on the characteristics of building blocks inside the clusters, such as the average number of building blocks (NBB) in a cluster and the average distance between the building blocks (inter-block chain length: IB-CL) can be estimated. Therefore, the building blocks give crucial information that indicates smaller unit structure of amylopectin (Bertoft, 2007a; X. Kong et al., 2009).

Most studies about the relationship between amylopectin microstructure and its impact on physical properties, which include gelatinization (Fredriksson et al., 1998; Gomand et al., 2010; Shi & Seib, 1992, 1995; Tziotis et al., 2005), pasting (Han & Hamaker, 2001; Tziotis et al., 2005), and gel textural properties (Hansen et al., 2008; Ong & Blanshard, 1995; Tziotis et al., 2005), have dealt with average chain length (CL) and chain length distribution of amylopectin as the chains group into different size-categories based on the report by Hanashiro et al. (1996).

As a polymer, starch can exhibit different properties influenced by chain flexibility, stiffness, geometric configuration, and branching of amylopectin

(Stevens, 1990). The amorphous regions in the granules also affect the physicochemical properties of the starch (Donovan, 1979; Genkina et al., 2007; Slade & Levine, 1988; Waigh et al., 2000). These demonstrate that the lamellar organization, polymer mobility and interaction of amylopectins are influenced by organization of chains in the amorphous lamella. In other words, the physical properties of starch are not simply related to the unit chain distribution of amylopectin.

There are some investigations relating the physicochemical properties of granular starches to the internal microstructure of amylopectin (Xiangli Kong et al., 2008; Vamadevan et al., 2013; Fan Zhu et al., 2011). However, these studies mostly focused on relationship with thermal properties of starch. Therefore, the objective of this study was to examine the relationship of the structural characteristics with the physical properties of waxy-cereal starches. For this purpose, the clusters of amylopectin and their building blocks were enzymatically isolated from four kinds of waxy-cereal (waxy corn, waxy rice, waxy barley, and waxy wheat) starches, and the unit organization was investigated by chromatographic methods. On the basis of these analyses, the effects of internal- and external-microstructural properties of amylopectin on the physical properties were studied.

# MATERIALS AND METHODS

## 1. Materials

### 1-1. Starch samples

Waxy rice (Hwaseonchalbyeo) and waxy barley (Hinchalssalbori) were purchased from Wonsam-Nonghyup (Yongin, Korea) and Chungmec Co. Ltd. (Gochang, Korea), respectively. Waxy wheat (Sinmichal) was provided by Hankook Woorimil-Nonghyup (Gwangju, Korea). Waxy corn starch was obtained from Ingredion Inc. (Westchester, IL, USA).

### 1-2. Enzymes

Rabbit muscle phosphorylase *a* (EC 2.4.1.1, 26 U/mg) was purchased from Sigma-Aldrich (St. Louis, MO, USA). All other enzymes, namely liquefying type of α-amylase from *Bacillus amyloliquefaciens* (EC 3.2.1.1, 160 U/mg), barley β-amylase (EC 3.2.1.2, 588 U/mg), isoamylase from *Pseudomonas* sp. (EC 3.2.1.68, 260 U/mg), and pullulanase from *Klebsiella planticola* (EC 3.2.1.41, 34 U/mg) were from Megazyme (Bray, Ireland).

## 2. Methods

### 2-1. Starch isolation

Except for waxy corn starch, waxy rice, waxy barley, and waxy wheat starches were extracted from grain.

Waxy rice and waxy barley starches were isolated using alkaline steeping method with slight modification described by Yang et al. (1984). After 24 h steeping in 0.2% sodium hydroxide, the grain was ground in a blender (HR2094, Koninklijke Philips N.V., Amsterdam, the Netherlands) at maximum speed for 3 min. The slurry was filtered through 35-, 50-, and 100-mesh sieves, and the suspension was collected in a plastic container. After the starch layer settled down, the supernatant was decanted, and the starch layer was dissolved in distilled water. The starch suspension was centrifuged at 7,000 × g for 10 min.

The grains of waxy wheat were milled with a blender, and sieved out. Waxy wheat starch was isolated from powdered wheat by using dough ball method with some modifications according to Alsberg and Rask (1924). The flour was mixed with 60 mL of distilled water per 100 g, and the dough was kneaded until the surface was smooth. Then it was kept at room temperature for 4 h. The dough was washed in excessive water by hand, and the solution was filtered through a 100-mesh sieve. The suspension was centrifuged at

1,000 × g for 10 min.

After centrifugation, the supernatant and the top yellowish layer of samples were removed, and the lower starch layer was resuspended in distilled water and centrifuged again (7,000 × g for waxy rice and waxy barley starches, 1,000 × g for waxy wheat starch, 10 min). This purification procedure was repeated until the surface looked completely white. The final pellet, prime starch, was dried at 40°C in a drying oven, ground, and passed through a 100-mesh sieve.

The amylose content of waxy corn, waxy rice, waxy barley, and waxy wheat starches were 2.21%, 2.28%, 1.68%, and 2.18%, respectively, determined with an amylose/amylopectin assay kit (Megazyme) based on the concanavalin A method (Gibson et al., 1997).

**2-2. Time course of α-amylolysis for cluster production from starches**

The structural analysis was conducted according to the method described by Bertoft et al. (2012a). Starches (400 mg) were dissolved in 8 mL of 90% dimethyl sulfoxide (DMSO) with constant stirring overnight, and then 28 mL of warm distilled water was added. After cooling, 4 mL of α-amylase (0.9 U/mL) in 0.01 M sodium acetate buffer (pH 6.5) was added to start the reaction in a water bath (25˚C) with magnetic stirring. The concentrations for starch and α-amylase in the reaction system were 10 mg/mL and 0.09 U/mL,

respectively. Samples (0.5 mL) were taken at 15, 30, 60, 120, and 180 min, and 10 μL of 5 M NaOH was added and mixed to destroy the α-amylase. The mixtures of the α-amylolysates were filtered through a 0.45 μm membrane filter, and then analyzed by gel-permeation chromatography (GPC) as describe below.

**2-3. Production of clusters from starches**

The cluster preparation was performed in the same manner above. The starch samples were incubated with α-amylase for the appropriate time (90 min), and the reaction was ended by adding 0.5 mL of 5 M NaOH. After keeping the samples at room temperature for 1h, 5 volumes of methanol were added to precipitate the clusters. The solution was centrifuged at 1,800 × g for 20 min, the supernatant was removed, and the precipitate was rinsed with methanol and centrifuged again. This procedure was repeated twice, and the precipitates were lyophilized.

**2-4. Production of φ,β-limit dextrins from clusters**

The production of φ,β-limit dextrins was conducted following the method of Bertoft (2007b) with minor modifications. Samples of clusters (100 mg) were dissolved in 35.7 mL of distilled water. After that, 3.6 mL of 1.1 M sodium phosphate buffer (pH 6.8), 1.7 mL of 2.8 mM EDTA, and 9 mL of

freshly prepared phosphorylase *a* solution (52 U) were added. The solution was stirred overnight at 35°C, and the reaction was terminated in a boiling water bath for 5 min. The solution was filtered through a 5.0 μm filter and reduced to 8 mL by a rotary evaporator (EYELA N-1100, Tokyo Rikakikai Co. Ltd., Tokyo, Japan) at 60°C. The purification (removal of glucose-1-phosphate) was performed on two PD-10 columns (GE Healthcare, Uppsala, Sweden) coupled in series: 2 mL of sample was applied on the columns followed by 3 mL of distilled water, and the eluate was discarded. After that, 5 mL distilled water was added, and the sample flowed out was collected. The phosphorylysis and purification procedures were repeated, and collected solution was freeze-dried to produce φ-limit dextrins.

The φ-limit dextrins (60 mg) were dissolved in 20 mL of distilled water, and 7 mL of 0.01 M sodium acetate buffer (pH 6.0) and β-amylase (240 U) were added. The solution was stirred overnight at 35°C and then placed in a boiling water bath for 5 min to terminate the reaction. The solution was filtered through a 5.0 μm filter, reduced to 8 mL using rotary evaporation, and purified (removal of maltose) on PD-10 columns as described above. The β-amylolysis was repeated, and the produced φ,β-limit dextrin was finally lyophilized.

## 2-5. Analysis of φ,β-limit dextrins

The lyophilized φ,β-limit dextrins were dissolved in distilled water (3 mg/mL). To 300 μL sample was added 30 μL of 5 M NaOH, and the mixed sample was applied on GPC. Another 200 μL of dextrin solution was diluted with 200 μL of distilled water, and 50 μL of 0.01 M sodium acetate buffer (pH 5.5), 1 μL of isoamylase, and 2 μL of pullulanase were added. The debranching reaction was conducted for 24 h at 35°C with constant stirring, the debranched samples were filtered through a 4.5 μm filter, and unit chain length profile was obtained by high-performance anion-exchange chromatography (HPAEC).

## 2-6. Characterization of building blocks in φ,β-limit dextrins

φ,β-Limit dextrins (3 mg) were dissolved in 540 μL of distilled water, and 60 μL of 60 U/mL α-amylase in 0.01 M sodium acetate buffer (pH 6.5) was added. The α-amylolysis was conducted at 35°C for 3 h and terminated in a boiling water bath for 5 min. After cooling, 60 μL of 0.01 M sodium acetate buffer (pH 6.0) and β-amylase (60 U) were added to the solution. The β-amylolysis was carried out at 35°C for 24 h, after which it was boiled again for 5 min. Afterward, 30 μL of 5 M NaOH was added to 300 μL of sample and it was analyzed on GPC.

## 2-7. Determination of unit chain length distribution by high-performance anion-exchange chromatography with pulsed amperometric detection (HPAEC-PAD)

The branch chain length distributions of native waxy starches were determined after the debranching of starches with isoamylase. Starch (15 mg) was dispersed in 3 mL of 90% DMSO and boiled for 30 min. Ethanol (15 mL) was added to the starch suspension to precipitate starch and centrifuged at 10,000 x g for 10 min. Then distilled water (1.5 mL) was added to the pellet and boiled for 15 min. After boiling, 1.5 mL of 50 mM sodium acetate buffer (pH 4.3) was added and boiled for 20 min. Isoamylase (30 μL) was added to the starch dispersion, and the sample was incubated at 45 °C and 30 rpm for 2 h in a water bath. Enzyme reaction was stopped by boiling for 10 min. Debranched sample was filtered through a 0.45 μm membrane filter and analyzed using HPAEC-PAD on a Carbo-pack PA1 anion-exchange column (4x250 mm, Dionex Corp., Sunnyvale, CA, USA) with a pulsed amperometric detector. The sample was injected at the initial 1 min, and eluted with a gradient of 600 mM sodium acetate in 150 mM NaOH with a flow rate 1 mL/min. The gradients of sodium acetate used were as follows: increasing from 0-20 % for 0-5 min, 20-45 % for 5-30 min, 45-55 % for 30-60 min, 55-60 % for 60-80 min, 60-65 % for 80-90 min, 65-80 % for 90-95 min, and 80-100 % for 95-100 min.

For φ,β-limit dextrins, the gradients of sodium acetate was slightly changed as follows: the gradients of sodium acetate used were increased from 0-20 % for 0-5 min, 20-25 % for 5-20 min, 25-55 % for 20-70 min, 55-60 % for 70-90 min, 60-65 % for 90-100 min, 65-80 % for 100-105 min, and 80-100 % for 105-110 min.

The values of DP were designated using a mixture of maltooligosaccharides (DP 1-7, Sigma–Aldrich Chemical Co., St. Louis, MO, USA) as standard. PeakNet software (version 5.11, Dionex) was used for calculation of peak areas.

**2-8. Analysis of molecular weight distribution by gel-permeation chromatography**

The molecular weight distribution of α-dextrins and their φ,β-limit dextrins, and building blocks were analyzed by GPC. The measurements were performed on high-performance liquid chromatography (HPLC) Ultimate 3000 system (Dionex Corp.) equipped with a refractive index (RI) detector. Ultrahydrogel 120, 500, and 1000 columns were connected in series, and 0.1 M sodium azide solution was used as the eluent at a flow rate of 1 mL/min at 40 °C. Pullulan standards (Mw 324–805000) were used to obtain a calibration curve. The system was controlled and the data were collected through Chromeleon 6.8 software package (Dionex Corp.).

## 2-9. X-ray diffraction patterns

X-ray diffraction was analyzed using a powder X-ray diffractometer (New D8 Advance, Bruker, Karlsruhe, Germany) at 40 kV and 40 mA. Starch sample scan was performed through 2θ range from 3° to 30° with a 0.02° step size and a count time of 2 sec. The relative crystallinity was determined by the following equation according to the method of Nara and Komiya (1983). The area was calculated using the software developed by the instrument manufacturer (EVA, 2.0).

$$\text{Relative crystallinity (\%)} = \left(\frac{\text{Crystalline area}}{\text{Total curve area}}\right) \times 100$$

## 2-10. Solid-state $^{13}C$ cross-polarization and magic-angle spinning (CP/MAS) nuclear magnetic resonance (NMR) spectra

A Bruker AVANCE 400 WB (Bruker) equipped with CP-MAS accessories was used for $^{13}C$ CP/MAS NMR analysis. Cross-polarization (CP), magic angle sample spinning (MAS), and high power decoupling conditions were used to observe NMR spectra (single scan). The acquisition time was 35 msec, time domain points, 2.2 k, and line broadening 10 Hz. The samples were spun at a rate of 5 kHz at room temperature in a 4 mm rotor with a spectral width of 3.1 kHz. Spectra were referenced to the high-field

resonance of adamantine (29.5 ppm).

The relative crystallinity (%) was calculated according to the method described by Paris et al. (1999). The percentage of relative crystallinity was calculated as the proportion of the fitting peak areas of the triplet (100-96 ppm) relative to the total area of the C1 spectrum (105-90 ppm).

**2-11. Measurement of thermal properties**

Thermal properties of the samples were investigated using a differential scanning calorimeter (DSC, Diamond DSC, Perkin-Elmer, Waltham, MA, USA). Each sample (10 mg, dry basis) was weighed in a hermetic aluminum pan (Seiko, Tokyo, Japan), and 30 μL of distilled water was added. The sample pan was sealed and kept at room temperature overnight for equilibrium. An empty aluminum pan was used as a reference, and indium was used for calibration. DSC scan was performed from 30 °C to 130 °C at 10 °C/min. The onset temperature ($T_o$), the peak temperature ($T_p$), the conclusion temperature ($T_c$), and the melting enthalpy ($\Delta H$) were recorded.

## 2-12. Analysis of pasting properties

Pasting properties of starch suspensions were measured with a Rapid Visco Analyzer (RVA-4, Newport Scientific Pty, Ltd., Warriewood, Australia). Each waxy starch (1.25g) was added to 25mL of distilled water. The starch suspension was equilibrated at 50°C for 1 min, heated from 50 to 95°C at a rate of 12°C/min, held at 95°C for 2.5 min, cooled to 50°C at the same rate, and held at 50°C for 2 min. The paddle speed was 960 rpm for the first 10 sec, then 160 rpm for the remainder of the experiment.

## 2-13. Measurement of rheological properties

The rheological properties of starch gel were measured using an oscillatory rheometer (Rheostress 1, Thermo HAAKE, Karlsruhe, Germany) with a cone-plate system (35 mm diameter, cone angle 1°, gap size 0.052 mm). A starch sample (100 mg) was dispersed with 1 mL of distilled water. The starch dispersion (10%, w/v) was boiled for 10 min and placed between the cone and plate in a rheometer. And then it was cooled to 25 °C for 10 min to form starch gel. After expelled materials were trimmed off, the sample at the edge of the system was covered by a thin layer of silicon oil to prevent drying. The frequency sweep measurement was carried out in a frequency range of 0.1-10 Hz at 25 °C. All measurement was performed in the linear viscoelastic region.

## 2-14. Statistical analysis

All the experiments were done in triplicate, and data were expressed as mean±standard deviation. Analysis of variance (ANOVA) was conducted and the mean separations were done by the Duncan's multiple range test at a significance level of 0.05. All the statistical analyses described above were conducted using PASW Statistic 18 (SPSS Corp., Chicago, IL, USA).

# RESULTS AND DISCUSSION

## 1. Branch chain length distributions of waxy-cereal starches

Hizukuri (1986) using GPC found that the chains of amylopectin possesse a characteristic periodicity in length. He subdivided the long chains into B2- (DP -45) and B3-chains (DP -70), which are involved in the interconnection of two or more clusters, respectively. The major group of short chains, mixture of short B1- and A-chains (DP -20), was suggested to build up clusters of chains. Later, using the new high-resolution technique of HPAEC, Hanashiro et al. (1996) categorized the unit chains of amylopectin into four fractions with shorter periodicity in chain length: fa with DP 6–12; $fb_1$ with DP 13–24; $fb_2$ with DP 25–36; $fb_3$ with DP >36. These researchers suggested that the fractions probably corresponded to A-, B1-, B2-, and B3-chains, although not agreeing with the older periodicity.

The branch chain length distribution and weight average DP of waxy-cereal starches are shown in Figure 1 and Table 1. All starches displayed two peaks, one is the large peak with DP 11-14 and the other is the relatively small peak at DP 40-45. The relative intensity of the peaks differed depending on kind of starches. In general, cereal starch, an A-type starch, has

larger proportions of short chains and smaller proportions of long chains (Hanashiro et al., 1996). Waxy rice starches (WRS) showed the largest portion of fa and had noticeable second peak due to the smallest portion of $fb_2$. Waxy corn starches (WCS) had the smallest portion of fa and the highest peak DP at 14. These results were in agreement with the previous report by Jane et al. (1999). The branch chain length distribution of waxy wheat starch (WWS) resembled that of waxy barley starch (WBS) showing a rapid increase of fa chains in the order of DP and sharp peak at DP 11. WBS and WWS also had broad distributions of $fb_1$ and $fb_2$ that caused blurred boundary with $fb_3$. Most starches displayed a shoulder around the first peak, and especially WBS and WWS showed an obvious shoulder at DP 20. On the other hand, WCS and WRS did not show a clear shoulder in the chromatogram. The shoulder may represent the full length of the crystallinity region (Cameron & Donald, 1992). Therefore, the ratio of the intensities of first peak and shoulder indicate the proportion of short chains in the crystallites that result defects (Jane et al., 1999). In general, diversity of amylopectin chain length distribution greatly influences amylopectin behavior in food systems and is an important factor determining functional properties (Zhang & Hamaker, 2012).

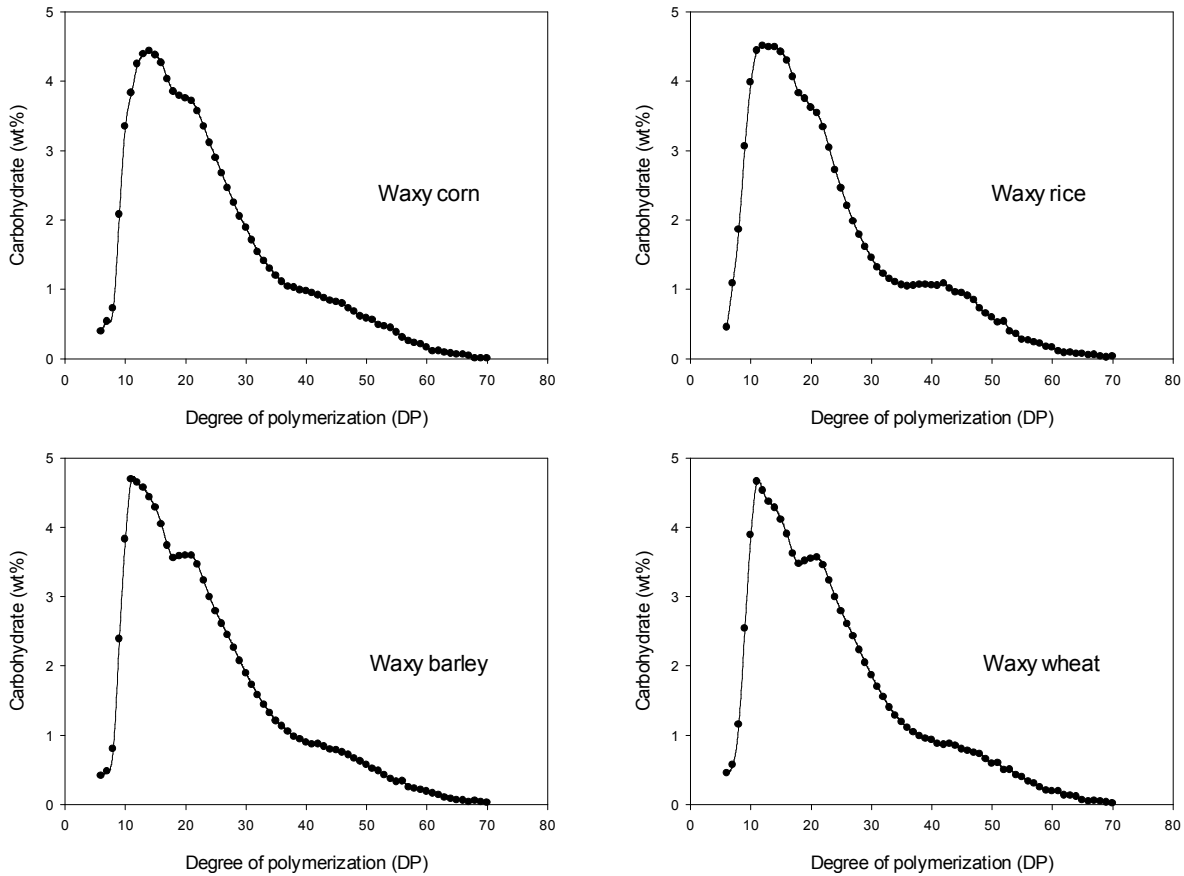


**Figure 1. Branch chain length distributions of waxy-cereal starches.**

**Table 1.**
**Proportions of branch chain categories of waxy-cereal starches**

| Samples | Percent distribution (%) | | | | $DP_w$ [2)] | Peak-DP[3)] |
|---|---|---|---|---|---|---|
| | fa[1)] | $fb_1$ | $fb_2$ | $fb_3$ | | |
| Waxy corn | 15.6±0.3$^{c}$ | 45.4±1.2$^{a}$ | 22.4±0.2$^{a}$ | 16.7±0.8$^{a}$ | 24.2±0.3$^{a}$ | 14 |
| Waxy rice | 18.8±1.0$^{a}$ | 44.4±1.5$^{a}$ | 19.3±1.0$^{b}$ | 17.6±1.5$^{a}$ | 23.6±0.7$^{a}$ | 12 |
| Waxy barley | 16.5±0.7$^{bc}$ | 43.9±1.8$^{a}$ | 23.5±0.9$^{a}$ | 16.2±1.7$^{a}$ | 24.1±0.7$^{a}$ | 11 |
| Waxy wheat | 17.3±1.0$^{b}$ | 42.8±1.4$^{a}$ | 22.8±1.0$^{a}$ | 17.1±1.3$^{a}$ | 24.3±0.6$^{a}$ | 11 |

[1)] Categories of chains: fa = DP 6-12, fb1 = DP 13-24, fb2 = DP 25-36, f b3 = DP ≥ 37 (Hanashiro et al., 1996)

[2)] Weigh-based average degree of polymerization (DP)

[3)] Peak-DP value from weigh-based average degree of polymerization

Data are expressed as average value and standard deviation.

The values with different superscripts in the same column are significantly different ($p < 0.05$).

## 2. Time course analysis of α-amylolysis of waxy-cereal starches

As a detailed investigation of cluster formation in waxy-cereal starches, proper time of α-amylolysis was determined using GPC. The changes in the molecular weight distribution with time are shown in Figure 2. The hydrolysis rates of all starch samples were rapid in the initial phase and then were slower, which is a universal feature of starch hydrolysis (Bertoft et al., 2011; X. Kong et al., 2009; F. Zhu et al., 2011). α-Amylolysis produced the distinct bimodal distribution of dextrins with all samples and at all hydrolysis time. The low molecular weight fraction (linear dextrins) contains small fragments derived primarily from external amylopectin chain and the high molecular weight fraction (branched dextrins) represents a cluster or groups of clusters. Zhu et al. (2013) found that the boundary between linear dextrins and branched dextrins from normal corn starch became less obvious. These researchers explained that it was caused by partially hydrolyzed amylose fragments. Such distinct distribution pattern in chromatograms suggested that the samples had little or no amylose and the results corresponded with amylose content of starches mentioned earlier.

The branched dextrins shifted to low molecular weight region over

hydrolysis time. Concurrently, the amount of linear dextrins that connect the clusters increased over time. The enzyme attacks simultaneously the external chains, resulting in the formation of predominantly maltohexaose fraction and long internal amylopectin chains, leading to the release of clusters (Robyt & French, 1963).

The average DP of branched dextrins, considered as cluster, was plotted against time in Figure 3. The hydrolysis rates differed depending on the kind of starches. WCS was hydrolyzed fastest and WRS had greatest resistance to α-amylase. However, the branched dextrin from all starches became more resistant to further attack by α-amylase after 90 min, and average DP of the branched dextrins leveled off around DP 100. Based on the time course analysis, 90 min was chosen to produce clusters under the conditions used in the current study.

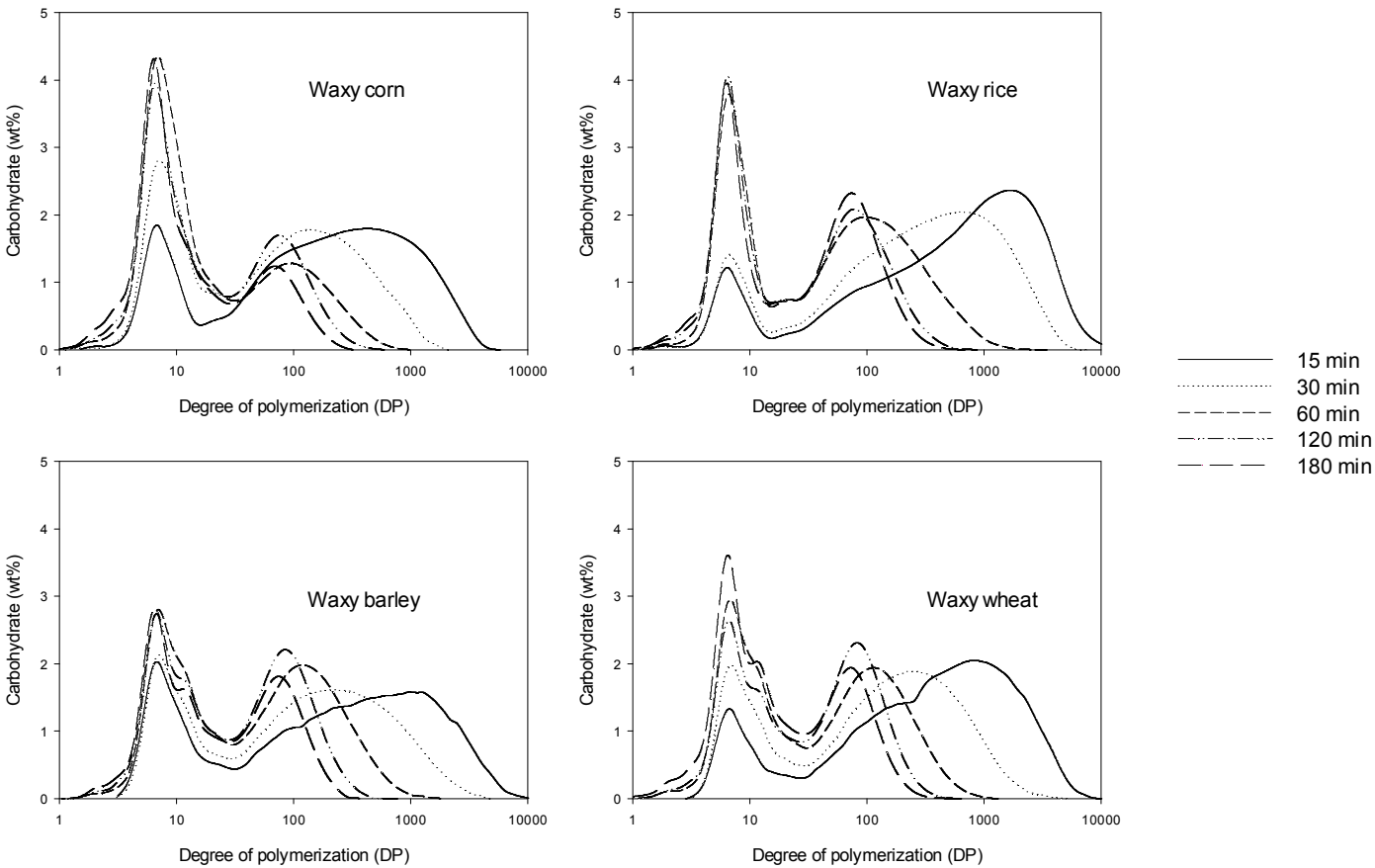


**Figure 2. Time course for α-amylolysis of waxy-cereal starches by gel-permeation chromatography.**

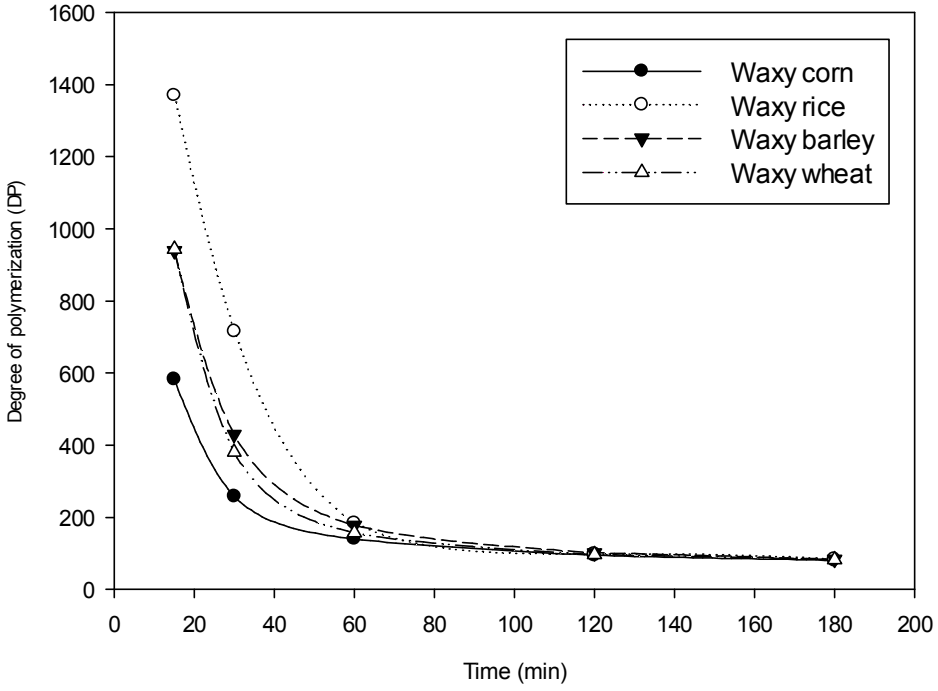


**Figure 3. Changes in average degree of polymerization of branched dextrins during α-amylolysis of waxy-cereal starches for cluster production.**

## 3. Characterization of clusters from waxy-cereal starches

Clusters in the form of α-dextrins were further characterized after phosphorylysis and β-amylolysis to remove external chains that remained following α-amylolysis. Average DP (avg DP) and peak-DP of φ,β-LDs are shown in Table 2. The smallest avg DP of φ,β-LD was obtained from WCS (80.5), while the largest one was from WRS (88.9). The avg DP of WBS and WWS were similar to each other. The same trend was also found for the peak-DP though its value was lower than avg DP. A similar result could also be observed in Figure 3. As mentioned above, the hydrolysis rate was the fastest and the slowest in the WCS and WRS, respectively. The difference in size of the cluster was also found in φ,β-LD implying that the φ,β-LDs of starches retain some structural properties of cluster in spite of phosphorylysis and β-amylolysis

The chain distribution of φ,β-LD is presented in Table 3 and Figure 4. When clusters are released, long chains in amylopectin are cleaved by α-amylase and new chains of shorter lengths are formed. As the new chains do not fit with the division of chains in the amylopectin (Hanashiro et al., 1996), a special nomenclature with small letters for the categories of chains in isolated clusters has been suggested (Bertoft et al., 2012a). Thus, it appears

that B3-chains in amylopectin are mostly hydrolyzed into b3-chains found in clusters (DP ≥ 28). Similarly, b2-chains in clusters formed by cleaved B2-chains, and these chains have a DP range between 19 and 27. Also, shorter chains (b1- and b0-chains, corresponding to DP 7–18 and 3–6, respectively) are produced when the clusters are released. Since all chains with maltosyl stub in φ,β-LD are a-chain, DP 2 chains are regarded as a-chain, However, some a-chains are also found as maltotriosyl residues due to their previous size reduction by α-amylase. Since β-amylase cannot hydrolyze the a-chains with maltotriose, it remains as DP 3. For this reason, the chains with DP 3 are regarded as a mixture of a- and b-chains. The relative distribution of DP 2 chain from WCS (52.7%) was far smaller than the others (56.2%-58.4%). Based on these values, calculated a- to b-chain ratios were 1.11, 1.38, 1.40, and 1.28 for WCS, WRS, WBS, and WWS, respectively. Considering a-chains in the DP 3 chains, this ratio could be increased slightly, and was in agreement with a previous report ranging between 0.8 and 1.5 (Manners, 1989). The ratios of b0-chains from WCS (10.1%) and WRS (9.5%) were similar, whereas WBS (8.0%) and WWS (7.4%) showed lower values. Boundary between b0- and b1-chains of WBS and WWS was clearly divided, and a shoulder was shown at DP 8. This shoulder was probably reflected in the shoulder at DP 20 in its original amylopectin (Figure 1).

CL estimated by HPAEC was greatly influenced by short chains of the

φ,β-LD being directly and inversely proportional to the chains with DP 2 and DP 3, respectively (Table 2 and 3). NC and peak-NC could be estimated as avg DP/CL and peak-DP/CL, respectively. Because cluster is formed binding short fa-chains with a fb-chain, NC in the cluster would be relative to the ratio of fa to fb-chains in amylopectin (Bertoft et al., 2012a). The lowest values of NC and peak-NC (12.7 and 10.8) came from WCS, while WRS (15.7 and 13.1) was higher than the others. These results were in accordance with the proportion of fa-chain in amylopectin (Table 1 and 2).

Longer CL automatically resulted in longer internal chain length (ICL), because the proportion between the external parts was almost similar in φ,β-LD. If the single external glucosyl residue is subtracted from the b-chains in the φ,β-LD, the total internal chain length (TICL) is obtained (Bertoft, 1991). This value was similar in samples ranging from 12.0 to 12.9. The TICL and the ICL values can be used to estimate the average number of chains carried by a b-chain (NC:b). Because ICL describes the average number of residues between those involved in the branches, and TICL is the length of the whole internal chain (including all residues involved in branches), NC:b is defined as TICL/(ICL + 1) (Bertoft et al., 2008). In WCS, the value of NC:b was lower (2.6) than that in any other sample. This particular φ,β-LD possessed the highest ICL value (4.2), suggesting a comparatively low branching density.

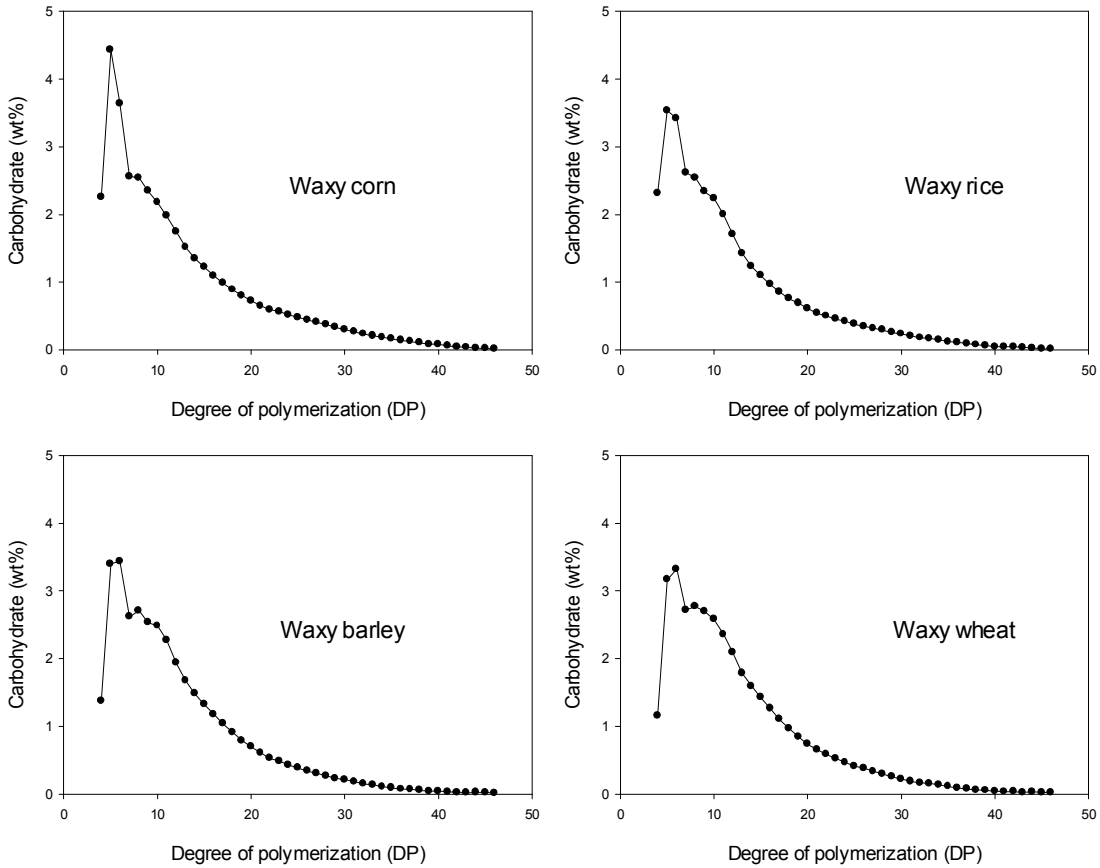


**Figure 4. Chain length distributions of limit dextrins from waxy-cereal starches.**

**Table 2.**
**Characterization of φ,β-limit dextrins of clusters from waxy-cereal starches**

| Samples | Avg DP[1)] | Peak-DP | NC[2)] | Peak-NC | DB (%)[3)] | CL[4)] | ICL[5)] | TICL[6)] | NC:b[7)] |
|---|---|---|---|---|---|---|---|---|---|
| Waxy corn | 80.5±1.4$^{c}$ | 68.1±2.4$^{b}$ | 12.7 | 10.8 | 14.6 | 6.3±0.1$^{a}$ | 4.2 | 12.9±0.1$^{a}$ | 2.5 |
| Waxy rice | 88.9±1.5$^{a}$ | 74.1±3.9$^{a}$ | 15.7 | 13.1 | 16.5 | 5.7±0.1$^{c}$ | 3.5 | 12.0±0.2$^{b}$ | 2.7 |
| Waxy barley | 85.1±1.9$^{b}$ | 73.3±3.2$^{ab}$ | 14.8 | 12.8 | 16.2 | 5.7±0.2$^{c}$ | 3.5 | 12.3±0.1$^{b}$ | 2.7 |
| Waxy wheat | 85.9±0.4$^{b}$ | 71.0±1.1$^{ab}$ | 14.3 | 11.8 | 15.5 | 6.0±0.1$^{b}$ | 3.8 | 12.8±0.4$^{a}$ | 2.7 |

[1)] Average DP and the peak position estimated by GPC

[2)] Number of chains estimated as avg DP/CL or peak-DP/CL

[3)] Degree of Branches (%) = (NC - 1)/avg DP x 100

[4)] Average chain length estimated by HPAEC

[5)] Internal chain length = (CL - ECL) x NC/(NC - 1) -1, in which ECL(External chain length) is 1.5.

[6)] Total internal chain length = CL of b-chains - 1

[7)] The average number of chains carried by a b-chain = TICL/ (ICL + 1)

Data are expressed as average value and standard deviation.

The values with different superscripts in the same column are significantly different ($p < 0.05$).

**Table 3.**
**Relative molar distribution of different chain categories in clusters isolated from waxy-cereal starches**

| Samples | DP 2[1)] | DP 3[2)] | DP ≥ 4[3)] | b0[4)] | b1 | b2 | b3 |
|---|---|---|---|---|---|---|---|
| Waxy corn | 52.7±1.4$^{b}$ | 8.4±1.0$^{a}$ | 38.9±0.5$^{a}$ | 10.1±0.5$^{a}$ | 20.7±0.2$^{a}$ | 5.1±0.2$^{a}$ | 3.0±0.4$^{a}$ |
| Waxy rice | 58.0±0.5$^{a}$ | 6.1±0.2$^{b}$ | 35.9±0.4$^{b}$ | 9.5±0.2$^{a}$ | 20.3±0.4$^{a}$ | 4.2±0.1$^{b}$ | 2.0±0.2$^{b}$ |
| Waxy barley | 58.3±1.3$^{a}$ | 6.0±0.2$^{b}$ | 35.7±1.1$^{b}$ | 8.0±0.2$^{b}$ | 21.6±0.6$^{a}$ | 4.4±0.2$^{b}$ | 1.7±0.1$^{b}$ |
| Waxy wheat | 56.2±1.9$^{a}$ | 7.6±0.4$^{a}$ | 36.2±2.2$^{b}$ | 7.4±0.3$^{b}$ | 21.9±2.2$^{a}$ | 4.9±0.2$^{a}$ | 2.0±0.2$^{b}$ |

[1)] a-Chains

[2)] Mixture of a- and b-chains

[3)] b-Chains

[4)] Categories of b-chains: b0 = DP 4-6, b1 = DP 7-18, b2 = DP 19-27, b3 = DP ≥ 28

Data are expressed as average value and standard deviation.

The values with different superscripts in the same column are significantly different ($p < 0.05$).

## 4. Characterization of building blocks in clusters of waxy-cereal starches

The molecular weight distributions of building blocks in clusters of waxy-cereal starches are displayed in Figure 5. Extensive hydrolysis of clusters with α-amylase releases building blocks, and linear dextrins with DP 1–6 are released from segments located between the branched blocks. These linear dextrins are further hydrolyzed into glucose, maltose, and maltotriose by treatment with β-amylase, a procedure that results in a better size separation of the linear products from the branched building blocks (Bertoft et al., 2012a). The molecular weight distribution of building block composition of waxy-cereal starches exhibited almost similar profiles. All chromatograms of hydrolysates exhibited two peaks. The first peak was linear dextrins hydrolyzed by β-amylase, and the second peak indicated the building blocks. The building block peak had a shoulder around at DP 7, and this represented group 2 building block. As described above, the building block profile was composed of regions representing the linear dextrins (group 1 with a peak at DP ～2) and the branched building blocks, which consist of groups 2, 3, and 4 containing 2, 3, and 4 chains, respectively (Bertoft et al., 2012b). Group 2 building block was most common, followed by group 3. WBS showed a

slightly higher amount of shoulder, and a relatively lower portion of linear dextrins peak was observed in WWS leading to a high amount of building block fragment in WBS and WWS.

Based on the molecular number and weight, the relative proportions of linear dextrins and building blocks and avg DP are presented in Table 4. The avg DP of building blocks was large in WRS (11.9) and WCS (11.5) whereas WBS (10.9) and WWS (10.7) had relatively small avg DP. The avg DP of linear dextrins was similar in all samples ranging from 2.1 (WCS, WRS, and WBS) to 2.3 (WWS). This was because the hydrolysates of β-amylolysis were mostly maltose and maltotriose.

The building block structure of the clusters is also shown in Table 4. The average number of branched building blocks (NBB) in a cluster ranged from 6.0 (WCS) to 7.2 (WWS). In the density of building blocks (DBB) in the clusters, a similar tendency was seen. DBB of WCS and WRS showed a lower value than that of WBS and WWS. The inter-block chain length (IB-CL) corresponding to the average chain length between two adjacent building blocks (Bertoft et al., 2012a) was calculated using the following equation:

$$\text{IB-CL} = \text{Mole\%}_{\text{linear}} \times \frac{\text{DP}_{\text{linear}}}{\text{Mole\%}_{\text{branched}}} + 4$$

In this equation, $Mole\%_{linear}$ and $DP_{linear}$ are the relative molar percentage and average DP of linear dextrins, respectively, and $Mole\%_{branched}$ is the relative molar percentage of branched building blocks. The number "4" relates to the two remaining glucose stubs on average in each of the adjacent building blocks based on the work by Umeki and Yamamoto (1972, 1975). The IB-CL of the samples was in inverse proportion to the DBB.

A higher NBB and short IB-CL found in WBS and WWS possibly increased the number of non-parallel double helices due to unfavorable combinations of spacer arms, and their short lengths decreased the flexibility of internal chains (Figure 6a). On the contrary, a lower NBB and long IB-CL, WCS and WRS, could facilitate the parallel alignment of external chains of amylopectin within the cluster (Figure 6b) (Vamadevan et al., 2013).

Due to the close alignment of strands, additional hydrogen bonds between double helices are established into crystallites and this interaction strengthens the crystal structure (Bogracheva et al., 2001). Besides intra-molecular organization of the double helices, the dimensions of crystallites in the starch granules suggest that they are organized through inter-molecular arrangements (Pérez & Bertoft, 2010).

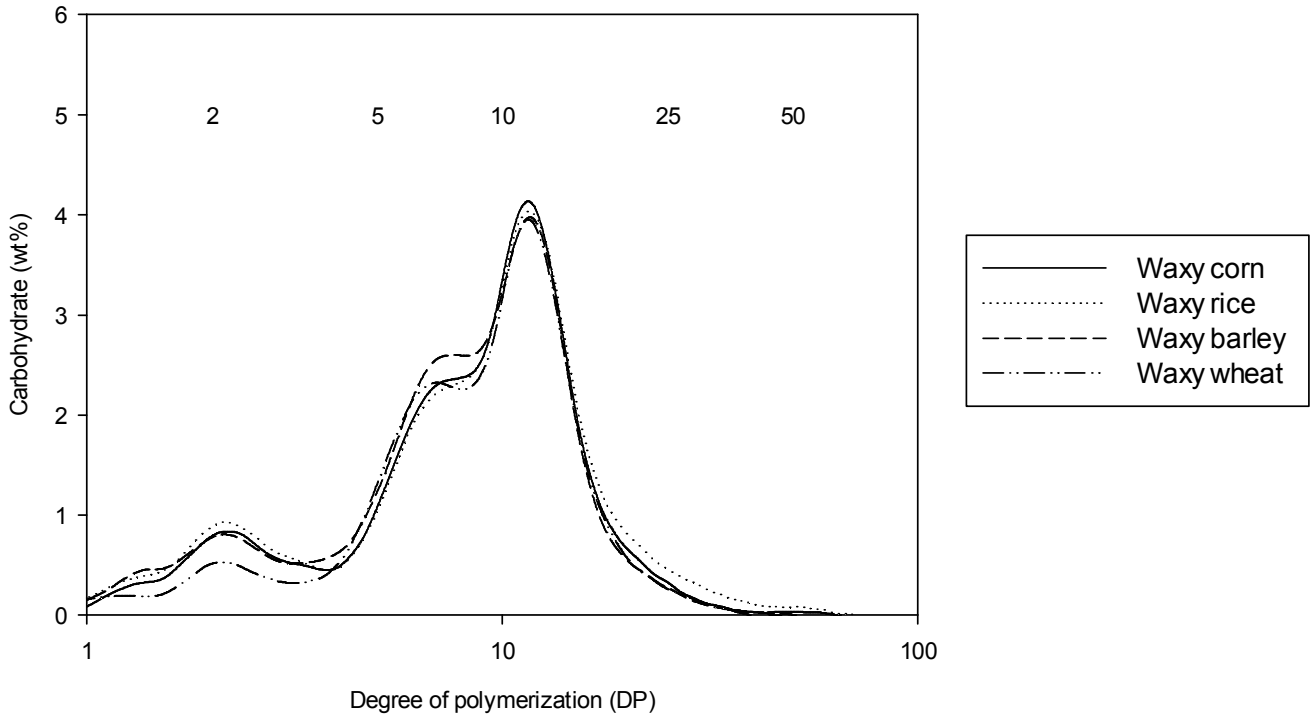


**Figure 5. Molecular weight distributions of building blocks in clusters of waxy-cereal starches.**

**Table 4.**
**Building block structure of clusters of amylopectin from waxy-cereal starches**

| Samples | Linear dextrins[1)] | | | Building blocks[2)] | | | NBB[3)] | DBB (%)[4)] | IB-CL[5)] |
|---|---|---|---|---|---|---|---|---|---|
| | Weight (%) | Mole (%) | DP | Weight (%) | Mole (%) | DP | | | |
| Waxy corn | 45.1±2.5$^{bc}$ | 45.1±2.5$^{bc}$ | 2.3±0.0$^{a}$ | 85.0±1.0$^{bc}$ | 54.9±2.5$^{bc}$ | 11.5±0.1$^{b}$ | 6.0 | 7.4 | 5.9 |
| Waxy rice | 47.8±1.7$^{c}$ | 47.8±1.7$^{c}$ | 2.3±0.0$^{a}$ | 84.0±0.8$^{c}$ | 52.2±1.7$^{c}$ | 11.9±0.0$^{a}$ | 6.3 | 7.1 | 6.1 |
| Waxy barley | 42.0±1.2$^{b}$ | 42.0±1.2$^{b}$ | 2.3±0.0$^{a}$ | 86.3±0.4$^{b}$ | 59.0±1.2$^{b}$ | 10.9±0.1$^{c}$ | 6.7 | 7.9 | 5.6 |
| Waxy wheat | 35.8±3.3$^{a}$ | 35.8±3.3$^{a}$ | 2.1±0.0$^{b}$ | 89.5±1.6$^{a}$ | 64.2±3.3$^{a}$ | 10.7±0.3$^{c}$ | 7.2 | 8.3 | 5.2 |

[1)] Low molecular peak fragments in Figure 5

[2)] High molecular peak dextrins in Figure 5

[3)] Average number of branched building blocks = (Weight%$_{BB}$/100) x ($DP_{\varphi,\beta\text{-}LD}/DP_{BB}$), (DP: degree of polymerization)

[4)] Density of building blocks = NBB/$DP_{\varphi,\beta\text{-}LD}$ x 100, (NBB: number of building blocks)

[5)] Inter-block chain length = (Mole%$_{\text{linear dextrins}}$ x $DP_{\text{linear dextrins}}$)/Mole%$_{BB}$ + 4

Data are expressed as average value and standard deviation.

The values with different superscripts in the same column are significantly different ($p < 0.05$).

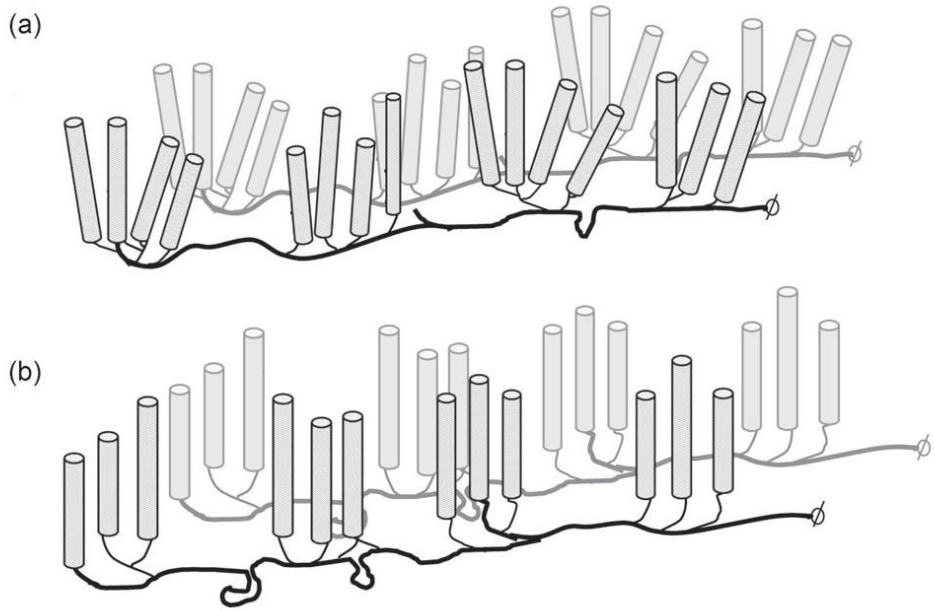


(Vamadevan et al. 2013)

**Figure 6. Schematic diagram for organization of double helices in the crystalline lamella through internal chain segments in the backbone of amylopectin:** Cylinders symbolize double helices, thick lines trace the backbone, and gray indicates another amylopectin molecule participating in the semi-crystalline arrangement in the starch granule. (a) Large clusters with high number of building blocks (NBB) in a cluster and short inter-block chain length (IB-CL) (b) Small clusters with less NBB in clusters and long IB-CL.

## 5. Relative crystallinity and disordered helix content

The different degrees of structural ordering of the starch are caused by the properties of crystallinity. The X-ray diffraction properties can give evidence of an ordered structure of the starch granule. When the starch granules are treated with acid or partially digested by amylases, the structure composed of concentric layers can be observed in electron microscope images (Buttrose, 1963; Palevitz & Newcomb, 1970). The crystallinity of the granules is mainly described as a function of the double helix formed by the branches of amylopectin (Hoover, 2001).

The crystalline structure is categorized according to its profile from a diffractogram using X-ray diffraction. Patterns known as types A, B and C represent specific diffraction angles caused by the double helix packing of the amylopectin branched chains (Parker & Ring, 2001). The pattern of crystallinity is defined on the basis of the relative intensity of the diffraction lines and interplanar spaces of the X-ray. A-type starch has strong diffraction peaks at about 15º and 23º, and an unresolved doublet at around 17º and 18º, and B-type starch gives the strong diffraction peak at around 5.6º and 17º, a few small peaks at around 15º, 20º, 22º, and 24º. C-type starch is a mixture of both A and B-type polymorphs (Cheetham & Tao, 1998).

The X-ray diffractograms of waxy-cereal starches are presented in Figure 7. All the waxy-cereal starches displayed peaks at 15.0º, 17.1º, 17.9º, and 23.0º, presenting the typical A-type X-ray patterns. Biliaderis (1991) reported that A-type pattern is characteristic of cereal starches, and B-type pattern is characteristic of starches from tubers, fruits, and high-amylose starch.

In spite of the similarity in X-ray diffraction pattern, significant differences were observed in the relative crystallinity (Table 5). WCS and WRS exhibited higher relative crystallinity (40.9% and 40.6%, respectively) than WBS (37.2%), and that of WWS (36.4%) was the lowest of any others.

Another analytical technique measuring the crystallinity is $^{13}C$ CP/MAS NMR. The $^{13}C$ CP/MAS NMR spectra of the waxy-cereal starches and amorphous starch are shown in Figure 8. Atichokudomchai et al. (2004) reported that the $^{13}C$ CP/MAS NMR spectrum for amorphous starch is not related to the type and method. Therefore, the amorphous starch was made with WCS by autoclaving and compared with waxy-cereal starches. All the waxy-cereal starches represented similar spectra, whereas amorphous starches exhibited somewhat different aspects. The C1 peak of the amorphous starch was shifted to the high field region (left side) following decreased signal at 100-96 ppm and increased signal at 105-100 ppm. Besides, higher intensity of C4 peak and lower intensity of C6 were also

observed in the spectrum of the amorphous starch. In $^{13}C$ CP/MAS NMR spectrum, the signals at 105-94 ppm, 85-81 ppm, and 65-58 ppm are attributed to C1, C4 and C6 in hexapyranoses, respectively, and the overlapping signals at 78-68 ppm are associated with C2, C3, and C5. The two broad shoulders that appear at 103 and 95 ppm can arise from the amorphous domains for C1 and the broad resonance of C4 peak is also regarded as amorphous domains (Atichokudomchai et al., 2004).

The crystallinity measured by $^{13}C$ CP/MAS NMR, ranging from 58.4% (WBS) to 60.4% (WCS), was much higher than that of X-ray diffraction (Table 5). Cooke and Gidley (1992) reported helices that are packed in regular arrays determine the crystallinity, which can be measured by both X-ray diffraction and $^{13}C$ CP/MAS NMR, while helices that are not packed in regular form or packed in the short-range distance cannot be detected by X-ray diffraction but can still be detected by $^{13}C$ CP/MAS NMR. For this reason, in general, the estimates of crystallinity by NMR spectroscopy are considerably higher than those obtained from X-ray diffraction. In this regard, the different crystallinity between X-ray and NMR might indicate that irregularly packed structure of double helices. The disordered helix contents are presented in Table 5. The values increased in the order: WRS (18.9%p), WCS (19.5%p), WBS (21.2%p), and WWS (22.6%p). This order was in accord with increasing and decreasing order of DBB and IB-CL,

respectively (Table 4). Moreover, higher values of WBS and WWS and lower values of WCS and WRS did not completely coincide with but were very similar to NBB. Hence, the disordered helix content represents splayed and non-parallel double helices, and it was proved once again that WBS and WWS had more irregularly packed double helices than WCS and WRS caused by densely located building blocks in amorphous lamella.

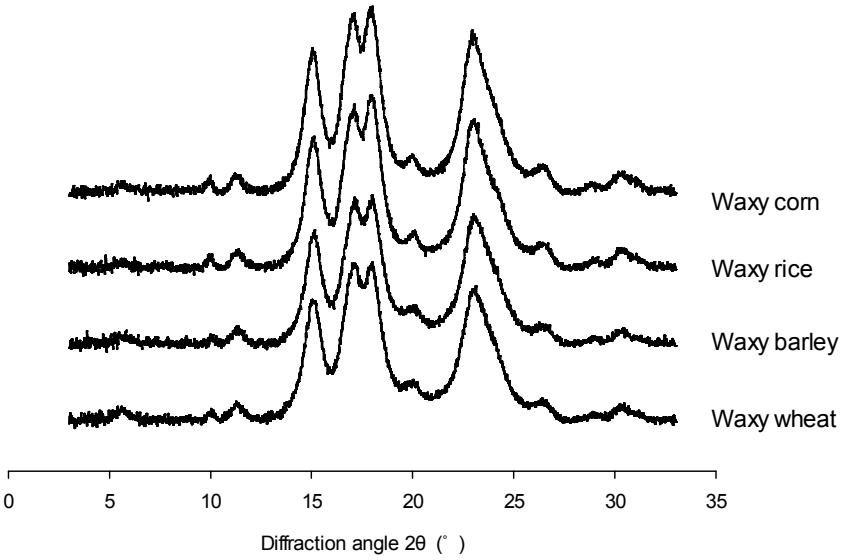


**Figure 7. X-ray diffraction patterns of waxy-cereal starches.**

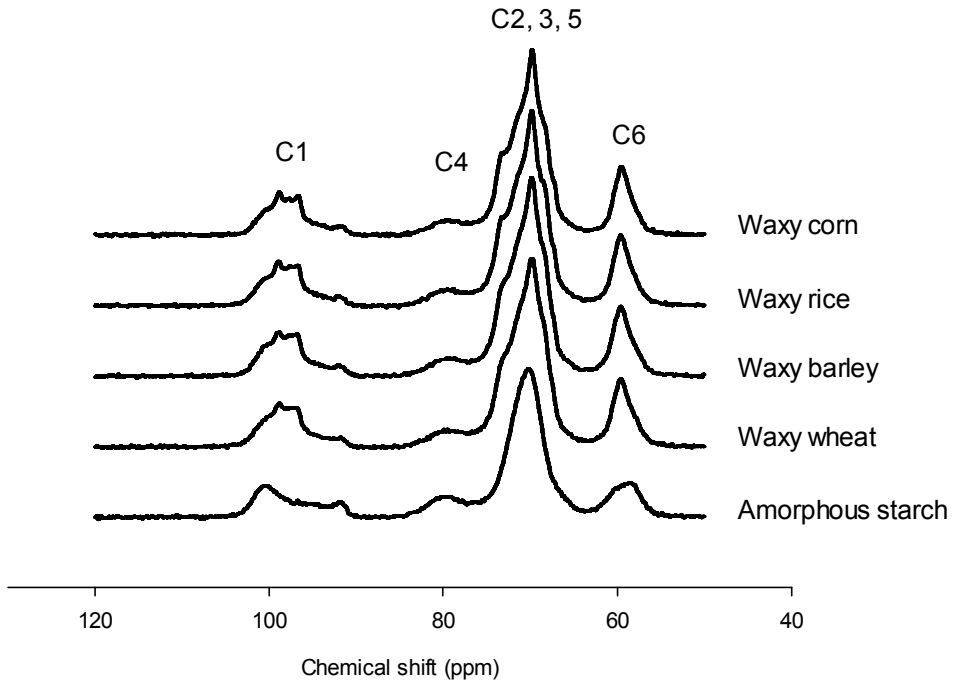


**Figure 8. $^{13}C$ CP/MAS NMR spectra of waxy-cereal and amorphous starches.**

**Table 5.**
**Relative crystallinity and disordered helix content of the waxy-cereal starches**

| Samples | Crystallinity (%) | | Disordered helix content (%p) [1)] |
|---|---|---|---|
| | X-ray | $^{13}$CP/MAS NMR | |
| Waxy corn | 40.9±0.1[a] | 60.4 | 19.5 |
| Waxy rice | 40.6±0.3[a] | 59.5 | 18.9 |
| Waxy barley | 37.2±0.3[b] | 58.4 | 21.2 |
| Waxy wheat | 36.4±0.5[c] | 59.0 | 22.6 |

[1)] Difference of crystallinity between X-ray diffraction and $^{13}$CP/MAS NMR

Data are expressed as average value and standard deviation.

The values with different superscripts in the same column are significantly different ($p$<0.05).

## 6. Thermal properties

When starch suspensions are heated in excess water and above a certain temperature, an irreversible transition called gelatinization which can be characterized by an endotherm obtained by DSC is caused. (Garcia et al., 1997). The gelatinization properties acquired by DSC analysis of the waxy-cereal starches are presented in Figure 9 and Table 6.

The thermal characteristics of each waxy-cereal starches were very unique. WRS showed the broadest temperature range caused by the highest peak temperature ($T_p$), whereas WWS had a significantly narrow temperature range (Figure 9). The transition temperature of WCS was high with the highest onset temperature ($T_o$) and $T_p$. In WWS, lowest $T_o$, $T_p$, and conclusion temperature ($T_c$) led to a low transition temperature. High transition temperatures in starch have been reported to result from a high quality of crystallinity, which provides structural stability and makes the granule more resistant towards gelatinization (Barichello et al., 1990). For this reason, gelatinization temperatures and enthalpies associated with gelatinization endotherms vary between the starches from different sources (Singh et al., 2003).

Both $T_o$ and $T_p$ increased in the order: WWS (57.1°C and 65.0°C), WBS (62.5°C and 67.0°C), WRS (64.7°C and 72.2°C), and WCS (65.3°C and 73.4°C) (Table 6). The order was identical to the decrease in NBB (Table 4). Tester (1997) has postulated that the extent of crystalline perfection is reflected in the gelatinization temperatures. In these results, it was verified that imperfect packing of double helices due to relatively large amount of building blocks in amorphous lamella provided the lower gelatinization temperature.

Gelatinization enthalpy ($\Delta H$) of WCS (11.5 J/g) and WRS (5.8 J/g) was higher and lower than the other starches, respectively. The $\Delta H$ was negatively correlated with short fa-chain in amylopectin ($r = -0.939$, $p < 0.05$) (Table 1). These phenomena are probably because short branches cannot participate in the crystallite formation and cause defects in the crystalline structure (Witt et al., 2012). Therefore, short fa-chains decrease the gelatinization temperature.

These results are in accordance with Vamadevan et al. (2013)'s study, who suggested that the length of the external chains of amylopectin has a large impact on melting enthalpy, and the internal structure of amylopectin in terms of unit chain organization has a major influence on gelatinization transition temperature.

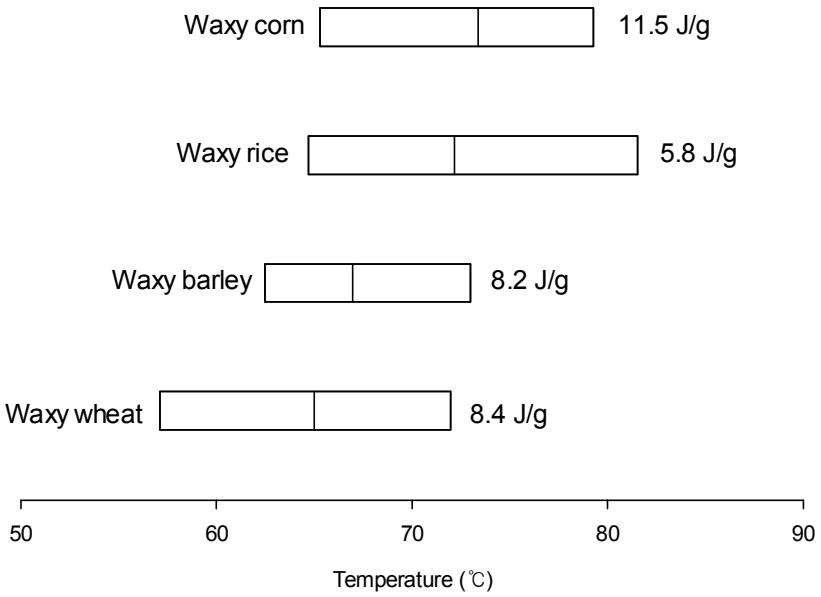


**Figure 9. Thermal parameters of waxy-cereal starches:** Bars indicate the temperature range of gelatinization ($T_o$-$T_c$) and border verifies the position of peak temperature.

**Table 6.**
**Gelatinization parameters of waxy-cereal starches**

| Samples | $T_o$ (°C)[1)] | $T_p$ (°C) | $T_c$ (°C) | $T_c$ - $T_o$ (°C)[2)] | $\Delta H$ (J/g)[3)] |
|---|---|---|---|---|---|
| Waxy corn | 65.3±0.1[a] | 73.4±0.2[a] | 79.3±0.2[b] | 14.0±0.2[c] | 11.5±0.2[a] |
| Waxy rice | 64.7±0.4[b] | 72.2±1.2[b] | 81.6±0.6[a] | 16.8±0.3[a] | 5.8±0.5[c] |
| Waxy barley | 62.5±0.1[c] | 67.0±0.2[c] | 73.0±0.2[c] | 10.5±0.2[d] | 8.2±0.1[b] |
| Waxy wheat | 57.1±0.2[d] | 65.0±0.1[d] | 72.0±0.0[d] | 14.9±0.1[b] | 8.4±0.2[b] |

[1)] $T_o$, $T_p$, and $T$c indicate the onset, peak, and conclusion temperatures of gelatinization, respectively.

[2)] The temperature range of gelatinization

[3)] The gelatinization enthalpy

Data are expressed as average value and standard deviation.

The values with different superscripts in the same column are significantly different ($p < 0.05$).

## 7. Pasting properties

The Rapid Visco Analyzer (RVA) is a rotational viscometer which is able to continuously record the viscosity of samples under controlled temperature and shear rate conditions. It is especially useful for flour or starch that requires a relatively complex test with varied temperature and shear rate (Wrigley et al., 1996). The swelling properties of starch are controlled in part by the molecular structure of amylopectin (unit chain length, extent of branching, molecular weight, and polydispersity), starch composition (amylose to amylopectin ratio), and granule architecture (crystalline to amorphous ratio) (Tester, 1997). The quality of starch-based product such as texture, stability, and digestibility is affected by the pasting properties (Han & Hamaker, 2001). Therefore, the pasting properties of starch are quite important for food industrial application.

Table 7 gives the pasting profiles of RVA of waxy-cereal starches displayed in Figure 9. WWS represented the highest peak viscosity (PV), trough viscosity (TV), and final viscosity (FV), and the viscosity characteristics of WBS were similar to those of WWS. On the contrary, WCS and WRS showed relatively low viscosities (PV, TV, and FV), very similar to each other. In RVA, a rise in viscosity during the initial heating phase

suggests that the granules begin to swell. A peak viscosity is obtained during pasting when there are a majority of fully swollen, intact granules and molecular alignment of solubilized polymers has not yet occurred. Thus, the higher viscosity reflects the higher swelling of granules. WWS showed the highest peak viscosity and relatively lower viscosity at the breakdown due to the irregular packing of double helices which promotes swelling and permits the increase in viscosity. If the double helices are less rigid, the water molecules may more easily penetrate into the granules and facilitate their swelling and disintegration during heating and shearing (Kozlov et al., 2007; Noda et al., 1998).

During the cooling phase, starch polymers begin to reassociate, and another rise in viscosity appears. This rise in viscosity is referred to as setback and indicates the retrogradation tendency. The relatively low setback of the all waxy-cereal starches represented little effect of amylopectin on starch retrogradation.

Peak time and pasting temperature in RVA mean the time when viscosity reaches the highest point and the temperature at viscosity begin to increase, respectively. The values of peak time were distinguished clearly: higher in WBS (5.1 min) and WWS (4.8 min) and lower in WCS (4.1 min) and WRS (4.0 min). The restricted swelling of WCS and WRS may be due to the bonding force between double helices caused by structure. Bonding forces

within the granules could affect their swelling behavior (Bahnassey & Breene, 1994). The strong bonding forces in WCS and WRS permitted more limited and slower swelling than the weaker bonding forces in WBS and WWS. The increased order of pasting temperature was identical with the $T_o$ in DSC (WWS < WBS < WRS < WCS). This close correspondence indicated that pasting temperature was influenced by the internal microstructure of amylopectin in the same way as $T_o$.

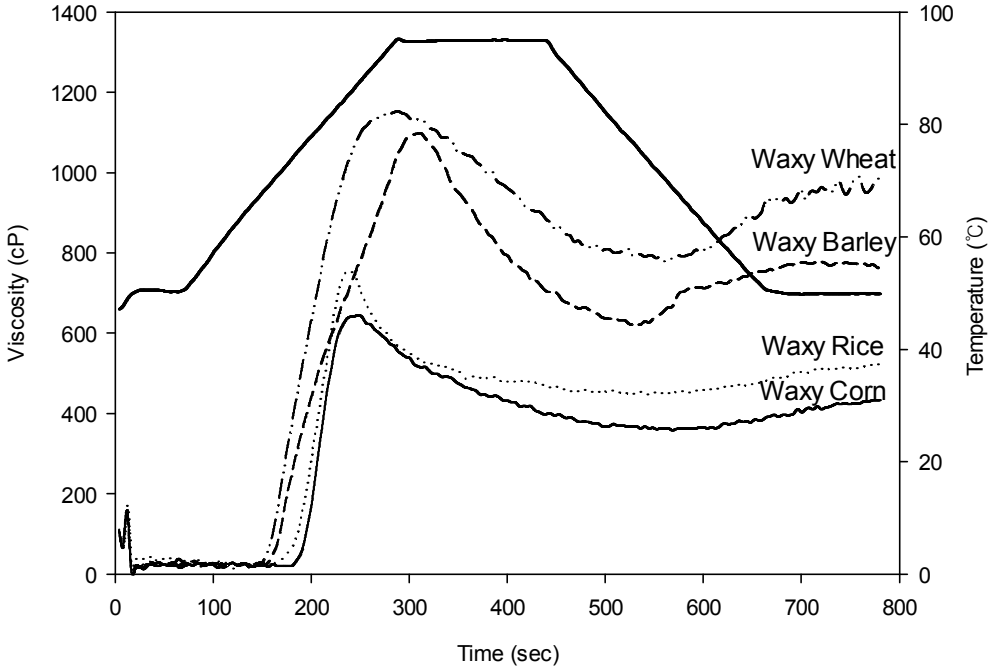


**Figure 10. Rapid Visco Analyzer pasting profiles of waxy-cereal starches.**

**Table 7.**
**Pasting properties of waxy-cereal starches**

| Samples | Viscosity (cP) | | | | | Peak time (min) | Pasting temperature (℃) |
|---|---|---|---|---|---|---|---|
| | Peak | Trough | Breakdown | Final | Setback | | |
| Waxy corn | 615.0±19.7$^{d}$ | 323.3±28.6$^{d}$ | 282.7±9.3$^{d}$ | 379.7±25.5$^{d}$ | 47.3±3.5$^{d}$ | 4.1±0.1$^{c}$ | 76.7±0.4$^{a}$ |
| Waxy rice | 743.0±22.2$^{c}$ | 399.7±2.5$^{c}$ | 343.3±24.5$^{c}$ | 489.3±5.8$^{c}$ | 89.7±6.0$^{c}$ | 4.0±0.0$^{c}$ | 75.8±0.5$^{b}$ |
| Waxy barley | 1083.0±12.3$^{b}$ | 614.3±9.3$^{b}$ | 468.7±10.1$^{a}$ | 776.0±14.1$^{b}$ | 161.7±19.7$^{b}$ | 5.1±0.0$^{a}$ | 71.4±0.4$^{c}$ |
| Waxy wheat | 1145.0± 8.0$^{a}$ | 768.7±9.8$^{a}$ | 376.3±4.9$^{b}$ | 963.3±19.6$^{a}$ | 194.7±11.4$^{a}$ | 4.8±0.1$^{b}$ | 70.1±0.1$^{d}$ |

Data are expressed as average value and standard deviation.

The values with different superscripts in the same column are significantly different ($p < 0.05$).

## 8. Rheological properties

Rheological properties of food materials are important not only in the texture and mouth feel but also in stability of the product (Muñtoz & Sherman, 1990). Most materials exhibit some viscous and some elastic behavior simultaneously and are called “viscoelastic”. Almost all foods, both liquid and solid, belong to this group. The viscoelastic properties of materials can be determined by dynamic methods. The frequency dependent functions G′ and G″ are shear elastic (storage) modulus and shear viscous (loss) modulus, respectively. G′ is a measure of the energy stored and the property relates to the molecular events of elastic nature. G″ is a measure of the energy dissipated as heat per cycle of deformation and characterizes viscous behavior of the polymer (Gunasekaran & Ak, 2000). Oscillation may be used to determine the strength and stability of a material. It gives an indication of the behavior of the sample, whether viscously or elastically dominated, over a given frequency range.

The mechanical spectra of the waxy-cereal starches are presented in Figure 11. G′ values were greater than G″ for all starch samples indicating that these waxy-cereal starch gels were more solid-like than liquid-like due to formation of starch gel from starch solution. All the starches represented

frequency dependence showing the increase in G′ and G″ with the increasing frequency over the entire frequency range. This frequency dependence suggests that the starch samples formed weak gels because of the absence of amylose. In general, chemical structure (DP ≥ 110) and physicochemical properties of amylose enable its macromolecules to form a gel network on cooling in which starch granules are embedded in a continuous network of amylose. In waxy starches, the phenomenon of gel formation is different from that of normal starch containing amylose. The building up of gel network in waxy starch may involve swollen granules alone (Byars et al., 2013; German et al., 1992; Hoover, 1995; Jane et al., 1999)

The G′ of starch gel was higher in WBS and WWS. In contrast, the G′ of WCS was the lowest, and WRS showed a similar value to WCS. This trend was in accord with the viscosity analyzed by RVA. Intermolecular associations can lead to the subsequent formation of junction zones and molecular aggregation in the developing gel networks. A well-known example of this gelation phenomenon is the retrogadation (Byars et al., 2013). Retrogradation is the reassociation of amylose and amylopectin to form double helices and crystalline structures, which is an important process that occurs during cooling storage of gelatinized starch (Hoover, 1995). Jane et al. (1999) reported that long amylopectin chains (DP > 50) accelerated retrogradation. A positive correlation between percent proportion of

amylopectin B-chains (DP > 40) and difference in values of G′ during cooling from 95˚C to 4˚C was observed by Chung et al. (2008). While no significant correlation between G′ and amylopectin chain-profile was found in this study, yet both long and short chains might not reassociate during this short period of time. Gel formation is largely dependent on short-term starch retrogradation due to formation of amylose double helices, and long-term retrogradation due to amylopectin (Lii et al., 2004). The waxy-cereal starches, having few or no amylose, need to longer time to retrograde. In starch gel, the movement of amylopectin is restricted due to its large molecular size at high viscosity. However, the linear amylose can leach from starch granules (Eliasson, 1986). Therefore, the gelation of waxy-cereal starches occurs with neighboring double helices at the early time. During swelling and heating, the original alignment of the amylopectin double helices collapses and simultaneously double helices dissociate. When recrystallization occurred, the double helices of WCS and WRS became isotropic array because long IB-CL caused less stiffness of chains. WCS and WRS further formed relatively weaker gels than WBS and WWS due to little junction zones and gel network in clusters. Keetels et al. (1996) gave two important postulations about the process of recrystallization of amylopectin in concentrated starch gels: (1) formation of crystalline clusters along the glucan chains in the amylopectin molecule, resulting in stiffening of strands

between entanglements, and (2) formation of cross-links between adjacent clusters. These strong gelling properties of WBS and WWS in short period of time can be used for specific foods requiring higher initial viscoelasticity but slow retrogradation.

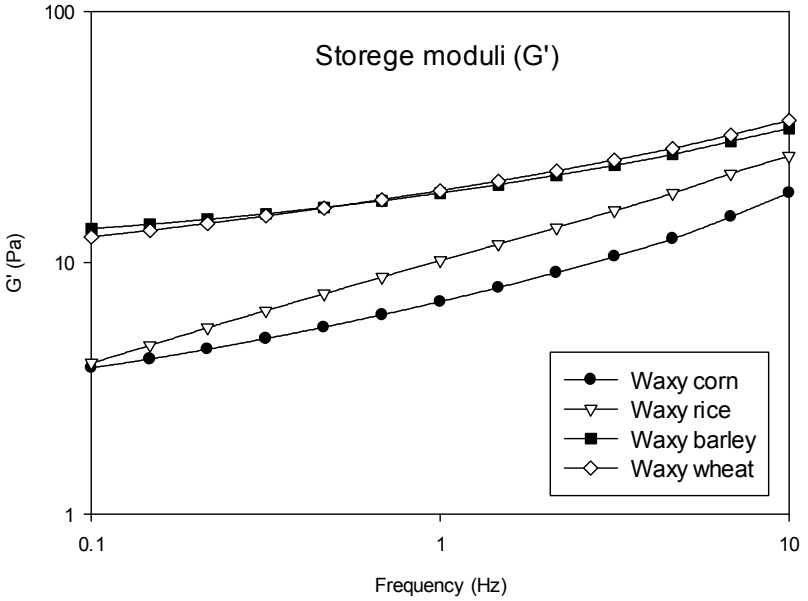


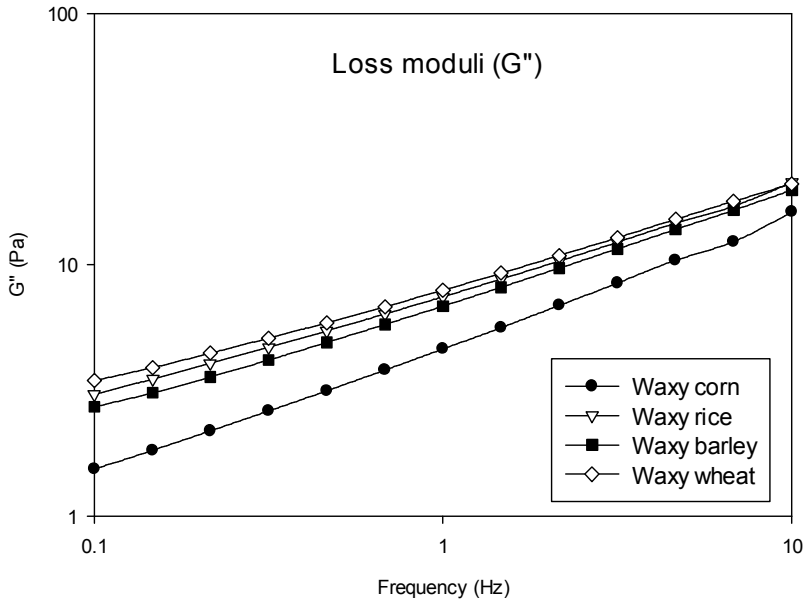


**Figure 11. Frequency dependence curves for gels of the waxy-cereal starches:** Storage moduli (G´) and loss moduli (G˝).

# CONCLUSION

In this study, the internal microstructures of four waxy-cereal amylopectins were investigated through partial hydrolysis into clusters and building blocks. The structural analysis with clusters and building blocks presented two types of distinguishable features. WCS and WRS showed a lower NBB and long IB-CL, whereas WBS and WWS had a higher NBB and short IB-CL. The X-ray diffraction patterns of the starches were similar, but the relative crystallinity was different. The disordered helix content expected from the value of relative crystallinity in X-ray diffraction and NMR was higher in WBS and WWS, but lower in WCS and WRS. It indicated that WBS and WWS had more irregularly packed double helices than WCS and WRS in amylopectin. Large clusters with high NBB and short IB-CL limited the parallel packing of double helices and contributed to a less perfect aligning of the amylopectin molecules. On the contrary, small clusters with less NBB and long IB-CL facilitated the parallel packing of adjacent double helices and allowed a more perfect aligning of the amylopectin molecules.

The effect of arrangement of double helices caused by internal microstructure was examined. The lower onset, peak, and pasting temperatures and high viscosity were observed in WBS and WWS because

less ordered double helices easily absorbed the water, swelled, and gelatinized. The higher gel elasticity in recrystallized WBS and WWS implied restricted movement of double helices due to short IB-CL.

These results suggest that internal microstructure of amylopectin can be used to describe unexplainable phenomena by the expectancy theory such as external branch chain distributions. Further studies on the characteristics of internal and external microstructures of amylopectin caused by starch biosynthesis may help understand more detailed microstructural features of starch. It would lead to the development of tailor-made starch ingredients for diverse food and non-food applications.

# REFERENCES


Alsberg, C., & Rask, O. (1924). On the gelatinization by heat of wheat and maize starch. *Experimental Biology and Medicine, 21*(8), 533-533.

Atichokudomchai, N., Varavinit, S., & Chinachoti, P. (2004). A study of ordered structure in acid-modified tapioca starch by $^{13}C$ CP/MAS solid-state NMR. *Carbohydrate Polymers, 58*(4), 383-389.

Bahnassey, Y. A., & Breene, W. M. (1994). Rapid visco-analyzer (rva) pasting profiles of wheat, corn, waxy corn, tapioca and amaranth starches (a. Hypochondriacus and a cruentus) in the presence of konjac flour, gellan, guar, xanthan and locust bean gums. *Starch-Stärke, 46*(4), 134-141.

Barichello, V., Yada, R. Y., Coffin, R. H., & Stanley, D. W. (1990). Low temperature sweetening in susceptible and resistant potatoes: Starch structure and composition. *Journal of Food Science, 55*(4), 1054-1059.

Bates, F. L., French, D., & Rundle, R. (1943). Amylose and amylopectin content of starches determined by their iodine complex formation1. *Journal of the American Chemical Society, 65*(2), 142-148.

Bertoft, E. (1989a). Investigation of the fine structure of amylopectin using alpha- and beta-amylase. *Carbohydrate Research, 189*, 195-207.

Bertoft, E. (1989b). Partial characterisation of amylopectin alpha-dextrins. *Carbohydrate Research, 189*, 181-193.

Bertoft, E. (1991). Investigation of the fine structure of alpha-dextrins derived from amylopectin and their relation to the structure of waxy-maize starch. *Carbohydrate Research, 212*, 229-244.

Bertoft, E. (2007a). Composition of building blocks in clusters from potato amylopectin. *Carbohydrate Polymers, 70*(1), 123-136.

Bertoft, E. (2007b). Composition of clusters and their arrangement in potato amylopectin. *Carbohydrate Polymers, 68*(3), 433-446.

Bertoft, E., Kallman, A., Koch, K., Andersson, R., & Aman, P. (2011). The cluster structure of barley amylopectins of different genetic backgrounds. *International Journal of Biological Macromolecules, 49*(4), 441-453.

Bertoft, E., Koch, K., & Åman, P. (2012a). Building block organisation of clusters in amylopectin from different structural types. *International Journal of Biological Macromolecules, 50*(5), 1212-1223.

Bertoft, E., Koch, K., & Åman, P. (2012b). Structure of building blocks in amylopectins. *Carbohydrate Research, 361*, 105-113.

Bertoft, E., Piyachomkwan, K., Chatakanonda, P., & Sriroth, K. (2008). Internal unit chain composition in amylopectins. *Carbohydrate Polymers, 74*(3), 527-543.

Bertoft, E., & Spoof, L. (1989). Fractional precipitation of amylopectin alpha-dextrins using methanol. *Carbohydrate Research, 189*, 169-180.

Bertoft, E., Zhu, Q., Andtfolk, H., & Jungner, M. (1999). Structural heterogeneity in waxy-rice starch. *Carbohydrate Polymers, 38*(4), 349-359.

Biliaderis, C. G. (1991). The structure and interactions of starch with food constituents. *Canadian Journal of Physiology and Pharmacology, 69*(1), 60-78.

Bogracheva, T. Y., Wang, Y., & Hedley, C. (2001). The effect of water content on the ordered/disordered structures in starches. *Biopolymers, 58*(3), 247-259.

Buttrose, M. (1963). Electron-microscopy of acid-degraded starch granules. *Starch-Stärke, 15*(3), 85-92.

Byars, J. A., Fanta, G. F., & Kenar, J. A. (2013). Effect of amylopectin on the rheological properties of aqueous dispersions of starch-sodium palmitate complexes. *Carbohydrate Polymers, 95*(1), 171-176.

Cameron, R., & Donald, A. (1992). A small-angle X-ray scattering study of the annealing and gelatinization of starch. *Polymer, 33*(12), 2628-2635.

Chanzy, H., Putaux, J.-L., Dupeyre, D., Davies, R., Burghammer, M., Montanari, S., & Riekel, C. (2006). Morphological and structural aspects of the giant starch granules from *phajus grandifolius*. *Journal of Structural Biology, 154*(1), 100-110.

Cheetham, N. W., & Tao, L. (1998). Variation in crystalline type with amylose content in maize starch granules: An X-ray powder diffraction study. *Carbohydrate Polymers, 36*(4), 277-284.

Chung, J.-H., Han, J.-A., Yoo, B., Seib, P., & Lim, S.-T. (2008). Effects of molecular size and chain profile of waxy cereal amylopectins on paste rheology during retrogradation. *Carbohydrate Polymers, 71*(3), 365-371.

Cooke, D., & Gidley, M. J. (1992). Loss of crystalline and molecular order during starch gelatinisation: Origin of the enthalpic transition. *Carbohydrate Research, 227*, 103-112.

Donovan, J. W. (1979). Phase transitions of the starch–water system. *Biopolymers, 18*(2), 263-275.

Eliasson, A. C. (1986). Viscoelastic behaviour during the gelatinization of starch i. Comparison of wheat, maize, potato and waxy-barley starches. *Journal of Texture Studies, 17*(3), 253-265.

Fredriksson, H., Silverio, J., Andersson, R., Eliasson, A.-C., & Åman, P. (1998). The influence of amylose and amylopectin characteristics on gelatinization and retrogradation properties of different starches. *Carbohydrate Polymers, 35*(3), 119-134.

Gallant, D. J., Bouchet, B., & Baldwin, P. M. (1997). Microscopy of starch: Evidence of a new level of granule organization. *Carbohydrate Polymers, 32*(3), 177-191.

Garcia, V., Colonna, P., Bouchet, B., & Gallant, D. J. (1997). Structural changes of cassava starch granules after heating at intermediate water contents. *Starch-Stärke, 49*(5), 171-179.

Genkina, N. K., Wikman, J., Bertoft, E., & Yuryev, V. P. (2007). Effects of structural imperfection on gelatinization characteristics of amylopectin starches with a-and b-type crystallinity. *Biomacromolecules, 8*(7), 2329-2335.

German, M. L., Blumenfeld, A. L., Guenin, Y. V., Yuryev, V. P., & Tolstoguzov, V. B. (1992). Structure formation in systems containing amylose, amylopectin, and their mixtures. *Carbohydrate Polymers, 18*(1), 27-34.

Gibson, T., Solah, V., & McCleary, B. (1997). A procedure to measure amylose in cereal starches and flours with concanavalin a. *Journal of Cereal Science, 25*(2), 111-119.

Gomand, S., Lamberts, L., Derde, L., Goesaert, H., Vandeputte, G., Goderis, B., Visser, R., & Delcour, J. (2010). Structural properties and gelatinisation characteristics of potato and cassava starches and mutants thereof. *Food Hydrocolloids, 24*(4), 307-317.

Gunasekaran, S., & Ak, M. M. (2000). Dynamic oscillatory shear testing of foods—selected applications. *Trends in Food Science & Technology, 11*(3), 115-127.

Han, X.-Z., & Hamaker, B. R. (2001). Amylopectin fine structure and rice starch paste breakdown. *Journal of Cereal Science, 34*(3), 279-284.

Hanashiro, I., Abe, J.-i., & Hizukuri, S. (1996). A periodic distribution of the chain length of amylopectin as revealed by high-performance anion-exchange chromatography. *Carbohydrate Research, 283*, 151-159.

Hansen, M. R., Blennow, A., Pedersen, S., Nørgaard, L., & Engelsen, S. B. (2008). Gel texture and chain structure of amylomaltase-modified starches compared to gelatin. *Food Hydrocolloids, 22*(8), 1551-1566.

Harada, T., Misaki, A., Akai, H., Yokobayashi, K., & Sugimoto, K. (1972). Characterization of *pseudomonas* isoamylase by its actions on amylopectin and glycogen: Comparison with *aerobacter* pullulanase. *Biochimica et Biophysica Acta (BBA)-Enzymology, 268*(2), 497-505.

Hizukuri, S. (1986). Polymodal distribution of the chain lengths of amylopectins, and its significance. *Carbohydrate Research, 147*(2), 342-347.

Hoover, R. (1995). Starch retrogradation. *Food Reviews International, 11*(2), 331-346.

Hoover, R. (2001). Composition, molecular structure, and physicochemical properties of tuber and root starches: A review. *Carbohydrate Polymers, 45*(3), 253-267.

Jane, J., Chen, Y., Lee, L., McPherson, A., Wong, K., Radosavljevic, M., & Kasemsuwan, T. (1999). Effects of amylopectin branch chain length and amylose content on the gelatinization and pasting properties of starch 1. *Cereal Chemistry, 76*(5), 629-637.

Jenkins, P. J., & Donald, A. M. (1997). The effect of acid hydrolyis on native starch granule structure. *Starch-Stärke, 49*(7-8), 262-267.

Kainuma, K., & French, D. (1972). Naegeli amylodextrin and its relationship to starch granule structure. Ii. Role of water in crystallization of b-starch. *Biopolymers, 11*(11), 2241-2250.

Keetels, C., Oostergetel, G., & Van Vliet, T. (1996). Recrystallization of amylopectin in concentrated starch gels. *Carbohydrate Polymers, 30*(1), 61-64.

Kong, X., Bertoft, E., Bao, J., & Corke, H. (2008). Molecular structure of amylopectin from amaranth starch and its effect on physicochemical properties. *International Journal of Biological Macromolecules, 43*(4), 377-382.

Kong, X., Corke, H., & Bertoft, E. (2009). Fine structure characterization of amylopectins from grain amaranth starch. *Carbohydrate Research, 344*(13), 1701-1708.

Kozlov, S., Krivandin, A., Shatalova, O. V., Noda, T., Bertoft, E., Fornal, J., & Yuryev, V. (2007). Structure of starches extracted from near-isogenic wheat lines. *Journal of Thermal Analysis and Calorimetry, 87*(2), 575-584.

Lii, C. Y., Lai, V. M. F., & Shen, M. C. (2004). Changes in retrogradation properties of rice starches with amylose content and molecular properties. *Cereal Chemistry, 81*(3), 392-398.

Muñtoz, J., & Sherman, P. (1990). Dynamic viscoelastic properties of some commercial salad dressings. *Journal of Texture Studies, 21*(4), 411-426.

Nara, S., & Komiya, T. (1983). Studies on the relationship between water-satured state and crystallinity by the diffraction method for moistened potato starch. *Starch-Stärke, 35*(12), 407-410.

Noda, T., Takahata, Y., Sato, T., Suda, I., Morishita, T., Ishiguro, K., & Yamakawa, O. (1998). Relationships between chain length distribution of amylopectin and gelatinization properties within the same botanical origin for sweet potato and buckwheat. *Carbohydrate Polymers, 37*(2), 153-158.

Ong, M., & Blanshard, J. (1995). Texture determinants in cooked, parboiled rice. I: Rice starch amylose and the fine stucture of amylopectin. *Journal of Cereal Science, 21*(3), 251-260.

Pérez, S., & Bertoft, E. (2010). The molecular structures of starch components and their contribution to the architecture of starch granules: A comprehensive review. *Starch-Stärke, 62*(8), 389-420.

Palevitz, B. A., & Newcomb, E. H. (1970). A study of sieve element starch using sequential enzymatic digestion and electron microscopy. *The Journal of Cell Biology, 45*(2), 383-398.

Paris, M., Bizot, H., Emery, J., Buzaré, J., & Buléon, A. (1999). Crystallinity and structuring role of water in native and recrystallized starches by $^{13}C$ CP-MAS NMR spectroscopy: 1: Spectral decomposition. *Carbohydrate Polymers, 39*(4), 327-339.

Parker, R., & Ring, S. (2001). Aspects of the physical chemistry of starch. *Journal of Cereal Science, 34*(1), 1-17.

Peat, S., Whelan, W., & Thomas, G. (1952). Evidence of multiple branching in waxy maize starch. In, (pp. 4546-4548): Royal Society of Chemistry, Thomas Graham House, Science Park, Milton Road, Cambridge CB4 0WF, England.

Robin, J. (1974). Lintnerized starches. Gel filtration and enzymatic studies of insoluble residues from prolonged acid treatment of potato starch. *Cereal Chemistry, 51*, 389-406.

Robyt, J., & French, D. (1963). Action pattern and specificity of an amylase from *bacillus subtilis*. *Archives of Biochemistry and Biophysics, 100*(3), 451-467.

Sasaki, T., Yasui, T., & Matsuki, J. (2000). Effect of amylose content on gelatinization, retrogradation, and pasting properties of starches from waxy and nonwaxy wheat and their f1 seeds. *Cereal Chemistry, 77*(1), 58-63.

Shi, Y.-C., & Seib, P. A. (1992). The structure of four waxy starches related to gelatinization and retrogradation. *Carbohydrate Research, 227*, 131-145.

Shi, Y.-C., & Seib, P. A. (1995). Fine structure of maize starches from four *wx*-containing genotypes of the w64a inbred line in relation to gelatinization and retrogradation. *Carbohydrate Polymers, 26*(2), 141-147.

Singh, N., Singh, J., Kaur, L., Singh Sodhi, N., & Singh Gill, B. (2003). Morphological, thermal and rheological properties of starches from different botanical sources. *Food Chemistry, 81*(2), 219-231.

Slade, L., & Levine, H. (1988). Non-equilibrium melting of native granular starch: Part i. Temperature location of the glass transition associated with gelatinization of a-type cereal starches. *Carbohydrate Polymers, 8*(3), 183-208.

Steup, M. (1988). Starch degradation. *The biochemistry of plants, 14*, 255-296.

Stevens, M. P. (1990). *Polymer chemistry*: Oxford University Press New York.

Takeda, Y., Shibahara, S., & Hanashiro, I. (2003). Examination of the structure of amylopectin molecules by fluorescent labeling. *Carbohydrate Research, 338*(5), 471-475.

Tester, R. (1997). Starch: The polysaccharide fractions. *Starch: structure and functionality*.

Tziotis, A., Seetharaman, K., Klucinec, J. D., Keeling, P., & White, P. J. (2005). Functional properties of starch from normal and mutant corn genotypes. *Carbohydrate Polymers, 61*(2), 238-247.

Umeki, K., & Yamamoto, T. (1972). Enzymatic determination of structure of singly branched hexaose dextrins formed by liquefying αamylase of bacillus subtilis. *Journal of Biochemistry, 72*(1), 101-109.

Umeki, K., & Yamamoto, T. (1975). Structures of singly branched heptaoses produced by bacterial liquefying α-amylase. *Journal of Biochemistry, 78*(5), 889-896.

Vamadevan, V., Bertoft, E., & Seetharaman, K. (2013). On the importance of organization of glucan chains on thermal properties of starch. *Carbohydrate Polymers, 92*(2), 1653-1659.

Waigh, T. A., Gidley, M. J., Komanshek, B. U., & Donald, A. M. (2000). The phase transformations in starch during gelatinisation: A liquid crystalline approach. *Carbohydrate Research, 328*(2), 165-176.

Waigh, T. A., Hopkinson, I., Donald, A. M., Butler, M. F., Heidelbach, F., & Riekel, C. (1997). Analysis of the native structure of starch granules with X-ray microfocus diffraction. *Macromolecules, 30*(13), 3813-3820.

Witt, T., Doutch, J., Gilbert, E. P., & Gilbert, R. G. (2012). Relations between molecular, crystalline, and lamellar structures of amylopectin. *Biomacromolecules, 13*(12), 4273-4282.

Wrigley, C., Booth, R., Bason, M., & Walker, C. (1996). Rapid visco analyser: Progress from concept to adoption. *Cereal Foods World, 41*(1), 6-11.

Yang, C., Lai, H., & Lii, C. (1984). The modified alkaline steeping method for the isolation of rice starch. *Food Science, 11*, 158-162.

Zhang, P., & Hamaker, B. R. (2012). Banana starch structure and digestibility. *Carbohydrate polymers, 87*(2), 1552-1558.

Zhu, F., Bertoft, E., & Seetharaman, K. (2013). Characterization of internal structure of maize starch without amylose and amylopectin separation. *Carbohydrate Polymers, 97*(2), 475-481.

Zhu, F., Corke, H., Aman, P., & Bertoft, E. (2011). Structures of clusters in sweetpotato amylopectin. *Carbohydrate Research, 346*(9), 1112-1121.

Zhu, F., Corke, H., & Bertoft, E. (2011). Amylopectin internal molecular structure in relation to physical properties of sweetpotato starch. *Carbohydrate Polymers, 84*(3), 907-918.

# 국문 초록

아밀로펙틴은 아밀로스와 함께 녹말을 구성하는 물질로 포도당의 중합체가 가지로 연결된 특징을 보인다. 이러한 아밀로펙틴의 형태적 특징은 녹말의 성질에 큰 영향을 미치므로 아밀로펙틴의 구조를 파악하는 것은 녹말 연구에 있어서 중요한 사항이다. 아밀로펙틴은 가지 사슬의 묶음형태인 클러스터가 배열되어 구성된다고 알려져 있다. 이 연구에서는 대표적인 A형의 곡류녹말인 찰옥수수, 찹쌀, 찰보리, 찰밀 녹말을 알파 아밀레이스로 부분적으로 가수분해하여 클러스터를 분리하였다. 또한 이 클러스터를 더욱 가수분해하여 더 작고 가지점들이 밀집된 빌딩블록을 형성하여 분석함으로써 아밀로펙틴의 내부 미세구조를 확인하였다. 이 연구의 목적은 아밀로펙틴의 클러스터와 빌딩블록의 특성을 분석하여 아밀로펙틴의 내부 미세구조가 곡류녹말의 물리적 특징인 상대적 결정화도, 열적 특성, 페이스팅 특성, 유변학적 특성에 미치는 영향을 알아보는 데 있었다.

베타 아밀레이스와 포스포릴레이스에 의해 외부사슬이 제거된 아밀로펙틴 클러스터의 중합도는 시료들 간에 큰 차이가 없었으며 a와 b사슬의 비율은 1.11 (찰옥수수녹말)에서 1.40(찰보리녹말)의 범위를 나타냈다. 실험에 사용된 네 가지 곡류 아밀로펙틴의 내부 미세구조 특징은 두 가지로 분류할 수 있었다. 찹쌀과 찰옥수수의 클러스터 내부는 상대적으로 적은 빌딩블록의 개수와 작은 밀도, 긴 빌딩블록들 간의 거리를 보였고, 찰보리와 찰밀은 많은 양의 빌딩블록으로

이루어져 있으며 큰 밀도와 짧은 빌딩블록들간의 거리를 갖는 것으로 나타났다. 이를 통해 내부의 구조적 특징에 따른 외부 이중 나선의 배열구조의 차이를 예상할 수 있었다. X-선 회절과 고체 핵 자기공명 분광법을 통해 예상된 무질서한 이중나선의 양은 찰옥수수와 찹쌀에서 낮았고, 찰보리와 찰밀은 높았다. 이러한 결과로 찰보리와 찰밀은 상대적으로 많은 양의 빌딩블록이 짧은 거리로 연결되어 있는 내부 구조 때문에 외부의 이중 나선이 찰옥수수와 찹쌀보다 무질서하게 배열되어 있음을 알 수 있었다. 시차주사 열량계를 통한 호화개시온도와 피크온도에서도 무질서한 이중나선의 빠른 호화가 관찰되었으며, 이러한 결과는 신속 점도기를 이용해 얻은 페이스팅 온도, 동적 레오미터로 측정된 점탄성의 차이에서도 확인할 수 있었다.

이 실험을 통해 아밀로펙틴의 무정형 얇은 층에서의 빌딩블록의 밀도와 빌딩블록간의 거리가 이중 나선의 결정성 얇은 층의 배열에 영향을 주는 것을 확인하였다. 또한 이러한 내부 미세구조에 의한 이중 나선의 배열이 녹말의 물리적 특징의 차이를 야기함을 증명하였다.

**핵심어:** 찰곡류녹말, 아밀로펙틴, 무정형 얇은 층, 내부 미세구조, 클러스터, 빌딩블록, 물리적 특성,

**학번: 2013-21177**